Campus Bio-Medico, University of Rome

PhD course in

SCIENCE AND ENGINEERING FOR HUMAN AND THE ENVIRONMENT
Curriculum: *Biosciences*

XXXV cycle 2019-2020

Hazelnut skin: from food waste to nutraceutical source. An investigation on its chemical composition, protective role against Advanced Glycation End-products (AGEs)-induced damage and *in silico* screening analysis

Ludovica Spagnuolo

Coordinator
Prof. Giulio Iannello

Tutor
Prof.ssa Laura Dugo

20 March 2023

Index

Introduction

Bioactive food compounds, like polyphenols, are known for their positive effects on human health. Polyphenols are a large group of secondary metabolites in plants and are, therefore, present in the human diet. Interestingly, it has been reported that long-term consumption of a diet rich in polyphenols has a protective effect against several diseases. In addition to anti-inflammatory properties, many studies have confirmed that different polyphenol substances have antiglycation functions *in vivo* and *in vitro*.

Advanced glycation end-products (AGEs) derive from spontaneous modification of proteins or amino acids through reducing sugars during Maillard reaction or non-enzymatic glycation. Glycation and the accumulation of AGEs are known to occur during physiological aging, diabetes, chronic diseases and in the development of tumors. Elevated blood glucose or methylglyoxal levels in diabetic patients result in an increase of AGEs. Despite the antidiabetic therapeutic options currently available, new, effective, and safe interventions are urgently required, because diabetes mellitus (DM) is still considered a health emergency.

In this work we have characterized polyphenols-rich extract obtained from hazelnut skins, a food waste product. Qualitative and quantitative phenolic compounds contents and antioxidant capability were also determined for further studying their relationship with AGE-inhibitory activity.

We have evaluated the possible inhibitory effects on AGEs formation, the cytotoxic effect and capacity of our extract to protect THP-1 derived macrophages from AGEs-induced damage *in vitro*, demonstrating that hazelnut skin polyphenols extract (HSE) shows positive effect on cell viability. After treatment with AGEs, macrophages express a high level of pro-inflammatory cytokines and reactive oxygen species (ROS), while co-treatment with polyphenol extract led to reduced levels of both TNF-α and IL1-β cytokines and reduced ROS production.

To date, our studies suggest that polyphenols-rich extracts have positive effect although further analysis should be conducted to identify the molecular pathway involved in AGEs-polyphenols interaction.

Finally, we have characterized the interaction between some compounds in our hazelnut skin extract with glucose transporters of class I (GLUTs) to identify potential GLUT-targeting drugs, based on a combination of structural biology by bioinformatics analysis (molecular docking). Our studies, although preliminary, have revealed a possible interaction between glucose transporters and polyphenols, in agreement with studies in the literature.

This research was funded by “Soremartec Italia Srl” (Alba, Cuneo, Italy) to promote a waste product, hazelnut skin, with bioactive potential.

Chapter 1

1.1 Polyphenols

Nowadays, the positive correlation between consumption of plant food rich in bioactive components and good health is well known. During the last decade, much research focused on the role of plant food in health maintenance and prevention of chronic disease [1],[2].

Polyphenols are secondary metabolites of plants with good antioxidants activities that can neutralize undesired reactive oxygen species (ROS) and reactive nitrogen species (RNS) produced during metabolic processes in the body [3]. These natural compounds show a broad range of biological activities as anti-inflammatory and anti-apoptotic activities, inhibition of α-amylase and glucosidase [4],[5],[6]. Furthermore, a diet rich in plant foods improve a diversity of intermediary markers of cardio metabolic risk, including blood pressure, glucose–insulin homeostasis, blood lipids and lipoproteins, endothelial function [7] and also to modulate functionality of the gut microbiota with a beneficial impact for human health [8].

There are different classes of polyphenols that share structural features of an aromatic ring and at least one hydroxyl group, classified by their chemical structures in phenolic acids, flavonoids, , stilbenes and lignans (figure 1) [9],[10].

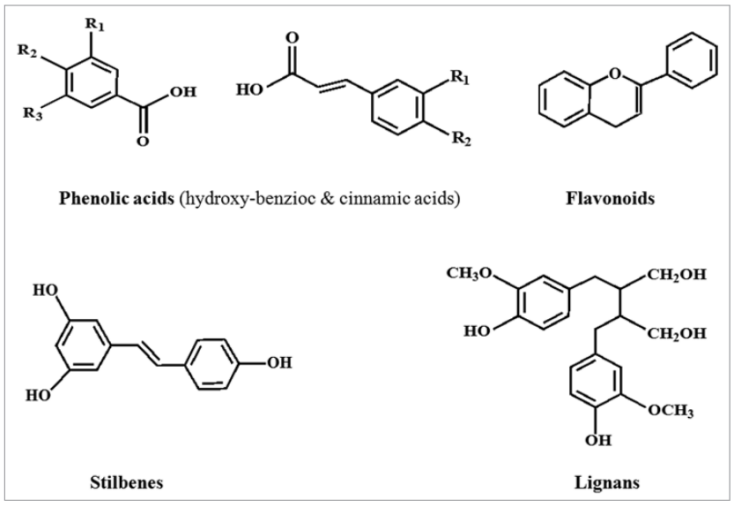

A)

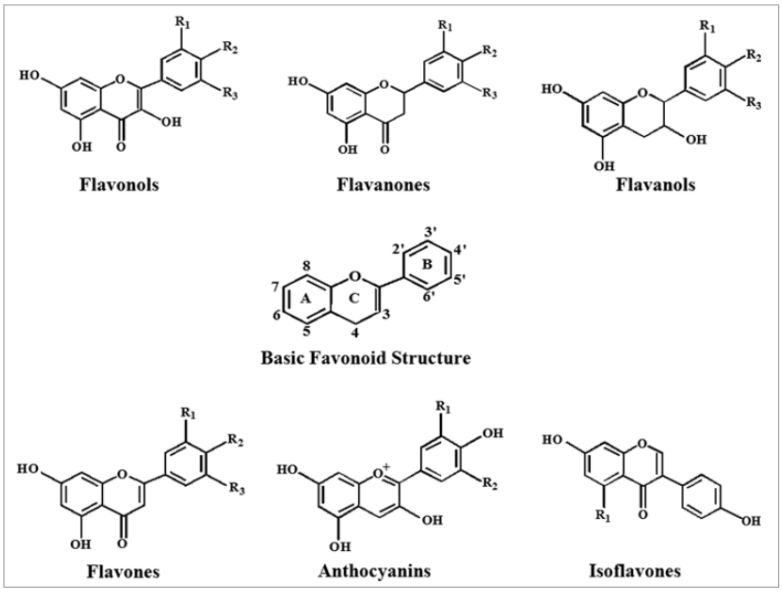

B)

Figure 1. A) Chemical structures of the different classes of polyphenols. **B)** Chemical structures of sub-classes of flavonoids. Pandey, K.B.; Rizvi, S.I. Plant Polyphenols as Dietary Antioxidants in Human Health and Disease. *Oxid Med Cell Longev* 2009

Phenolic acids account for about a third of the polyphenolic compounds in our diet and are found in all plant material, but are particularly abundant in acidic-tasting fruits. Caffeic acid, gallic acid, ferulic acid are some common phenolic acids. Flavonoids are most abundant polyphenols in human diet and share a common basic structure consist of two aromatic rings, which are bound together by three carbon atoms that form an oxygenated heterocycle. Stilbenes contain two phenyl moieties connected by a two-carbon methylene bridge. The most extensively studied stilbene is resveratrol; lignans are di-phenolic compounds that contain a 2,3-dibenzylbutane structure that is formed by the dimerization of two cinnamic acid residues [11]. Based on the variation in the type of heterocycle involved, flavonoids are divided into six major subclasses: flavonols, flavanones, flavanols, flavones, anthocyanins and isoflavones. Individual differences within each group arise from the variation in number and arrangement of the hydroxyl groups and their extent of alkylation and/or glycosylation. Flavonols (such as quercetin and kaempferol), have a 3-hydroxy pyran-4-one group on the C ring, flavanones (such as naringenin and taxifolin) have an unsaturated carbon-carbon bond in the C ring, flavanols (such as the catechins) lack both a 3-hydroxyl group and the 4-one structure in the C ring and flavones (such as luteolin) lack a hydroxyl group in the 3-position on the C ring. Anthocyanins, such as cyanidin, are characterized by the presence of an oxonium ion on the C ring and are highly coloured as a consequence and in isoflavones (such as genistein), the B ring is attached to the C ring in the 3-position, rather than the 2-position as is the case with the other flavonoids [12].

The bioavailability of the polyphenols present in foods is often very low. Thus, most of the dietary polyphenols reach the colon unmodified, where they interact with the commensal microbiota, being catabolized to provide relevant metabolites that are better absorbed and that show consistent biological effects [13].

The bioavailability of each polyphenol is different, but there is no relation between the quantity of polyphenols in food and their bioavailability in human body. As a consequence, the forms reaching the blood and tissues are different from those present in food and it is very difficult to identify all the metabolites and to evaluate their biological activity [14]. Polyphenols also differs in their site of absorption in humans. Some of the polyphenols are well absorbed in the gastro-intestinal tract while others in intestine or other part of the digestive tract. Accumulation of polyphenols in the tissues is the most important phase of polyphenol metabolism because this is the concentration which is biologically active for exerting the effects of polyphenols. Studies have shown that the polyphenols are able to penetrate tissues. Thus the health beneficial effects of the polyphenols depend upon both the intake and bioavailability [15].

Phenolic compounds have been reported to have different beneficial effects on human health, such as antioxidant properties, and, as demonstrated in previous studies, also an anti-glycation function [16]. Indeed, a recently published review reports the inhibitory effects of polyphenols and plant extracts on the formation of advanced glycation end-products (AGEs) [17].

1.2 Hazelnut skin: a food waste product

According to the United Nation's Food and Agriculture Organization (FAO, 2019) [18] about 1.3 billion tons of food are wasted or lost each year worldwide. The phenolic compounds present abundantly in such residues have been successfully applied in different sectors, including the food industry, for the development of functional foods or supplements; the health industry, for medicines and pharmaceuticals and the cosmetic industry, among others [19]. Therefore, the recovery of active compounds from food waste residues can be an interesting strategy, because in addition to being a natural and safe source of polyphenols, they are inexhaustible, low cost, and sustainable resources [20]. Moreover, food waste products derived from food processing are still quite rich in interesting bioactive compounds, which could be extracted and used to produce nutraceutical supplements [21].

In this context hazelnuts represent an interesting source of by-products, producing a big amount of waste material such as leafy covers, skins, and shells. Hazelnuts are typically consumed whole or used as an ingredient in many processed foods. Recently, the study of their composition has gained attention with the aim to add economic value to waste from hazelnut processing. A wide investigation on hazelnut showed their antioxidant activity by different tests, revealing as they could potentially be

considered an excellent source of natural antioxidants. Recently published data indicated that roasted hazelnut skin is a richer source of total phenolics and has the highest antioxidant activity, followed by natural and roasted hazelnuts [22],[23]. The main bioactive molecules in hazelnut waste are phenol compounds and the skin is a richer source of these bio-active molecules, at least in quantitative terms [24],[25].

Moreover, hazelnut skin is an important by-product of the food industry, if we consider that more than 160,000 tons of hazelnuts are produced annually only by the Ferrero Hazelnut Company (https://www.hazelnutcompany.ferrero.com, accessed on 1 February 2021; Ferrero International S.A. Findel, Luxemburg). Worldwide hazelnut production in 2019/2020 was roughly 528,070 tons. Taking into account that roughly 67% of the total fruit weight is comprised of the shell leads to roughly 353,807 tons of hazelnut shells each year [26],[27]. Hazelnut skin represents 2.5% by weight of the raw material, and it is discarded upon roasting. It has been traditionally used as animal bedding, but a lot of research underlined its potentiality as a source of natural antioxidants and dietary fibers [28].

Indeed, hazelnut skin represents an interesting source of bioactive molecules for nutraceutical or food supplements production, in a circular economy approach. Valorization of products defined as "waste" can contribute to both solving the problem of waste management and disposal, with a considerable economic advantage for companies, other than being greatly environmental-friendly and offering a vast range of molecules of natural origin easily available and eco-sustainable.

1.3 Polyphenols as nutraceutical

The healthy and conscious daily intake of micro- and macronutrients plays a key role in humans' wellbeing. Food (unprocessed or processed, in whole or in its edible part) is a reserve of nutrients and substances with no nutritional relevance, namely nutraceutical compounds, with positive effects on human health [29]. According to the first definition of "The foundation for Innovation in Medicine" nutraceutical is a food or part of it that provides medical or health benefits, including the prevention or treatment of diseases [30]. For a long time, the intake of fruit and vegetable was associated with reduced risk of chronic and degenerative diseases onset. These findings are correlated to plants diversity and their richness in bioactive compounds, natural substances able to modulate one or more metabolic processes. Therefore, several scientific data supports the hypothesis that anti-oxidant phytochemicals in food and in their isolated pure form ensure health conditions [31],[32]. Indeed, polyphenols are able to prevent or massively slow-down oxidative stress related diseases, due to their intrinsic attitude to neutralize, deactivate or suppress free radical species, by donating an electron or hydrogen atom or, directly, to act as inhibitors of lipoperoxidation chain reaction [33]. Additionally,

agricultural by-products and food waste are natural sources of these food antioxidants, whose sustainable recovery, recycle and reuse is aimed at breaking down their environmental impact [34].

Nutraceuticals are gaining considerable attention due to their nutrition and therapeutic potentials. Based on their sources, they are classified as dietary supplements and plant-based bioactive compounds, which play a role in maintaining longevity, good health and quality of life [35].

Various *in vivo* and *in vitro* studies have been conducted to study the protective role of nutraceuticals against various diseases but it has not been clinically proved in many cases. From a toxicological point of view, nutraceuticals are usually safe at dietary doses, but their consumption in high doses can be toxic, mainly due to the presence of substances that may cause genomic changes in target tissues. So, it is important to take an optimum dose of any food item for health benefits [36].

For example, hazelnut is used in a wide range of applications with increased demands for them in the global markets, used mainly as a feedstock in the food industry, for example in the sweet sector. Moreover, hazelnut oil is used in cosmetic, medicinal and cooking products and hazelnut skin is used an ingredient in different processed foods like bakery and confectionery products [37]. The skin has good antioxidant activity and has been shown to have a potential role in disease prevention and treatment. Hazelnut consumption leads to an improvement in lipoprotein profile and α-tocopherol concentrations in mildly hypercholesterolaemic individuals, reducing the risk of cardiovascular disease (CVD). Furthermore, as hazelnuts are rich in polyphenols, they have high antioxidant potential, antimicrobial activity and reduce the risk of inflammatory diseases [38].

Considering these properties, hazelnut skin may have the potential to be developed as nutraceutical or dietary supplements.

Chapter 2

2.1 Advanced glycation end product (AGEs)

AGEs are heterogeneous compounds that derive from the reaction of reducing sugars with the free amino groups in proteins, nucleic acids, and lipids in a non-enzymatic Maillard-reaction [39].

The formation of AGEs occurs in three phases. First, glucose attaches to a free amino acid (mainly lysine and arginine) of a protein, lipid or DNA to form a Schiff base, a compound that has a carbon to nitrogen double bond where the nitrogen is not connected to hydrogen. The initiation of this first step depends on glucose concentration, takes place within hours and the reaction is reversible. During the second phase, the Schiff base undergoes chemical rearrangement over a period of days and form Amadori products (also known as early glycation products). The Amadori products are more stable compounds (for example hemoglobin A1c is the most well-known), but the reaction is still reversible. If there is accumulation of Amadori products, they will undergo complicated chemical rearrangements (oxidations, reductions, and hydrations) and form crosslinked proteins. This process takes place in weeks or months and it is irreversible. The final brownish products are called AGEs and some of them have fluorescent properties. They are very stable, and accumulate inside and outside the cells and interfere with protein function [40].

In addition, lipid and amino acid degradation, cleavage of di-carbonyl compounds from aldimins (Namiki pathway) as well as the formation of carbonyl compounds after autoxidation of monosaccharaides, such as glucose, ribose, fructose and glyceraldehyde (Wolff pathway) generate AGE precursor compounds and result in the formation of stable AGEs (figure 2) [41].

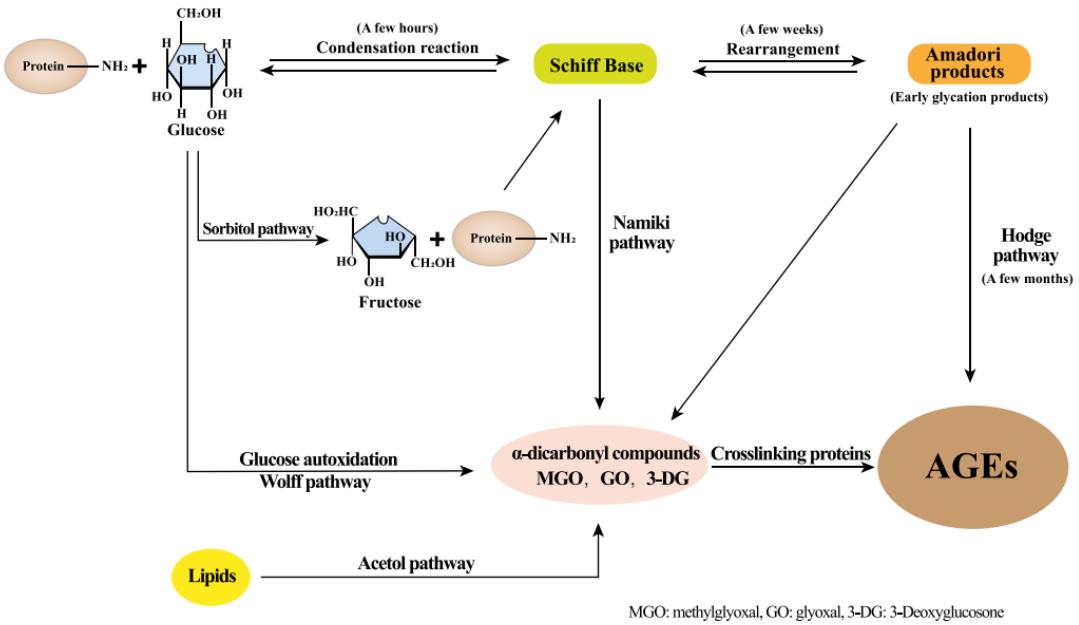

Figure 2. Formation of AGEs. Glucose and proteins produce Schiff bases through reversible reactions and finally Amadori products. Some Amadori products are converted to AGEs, and others are oxidized and cleaved to active dicarbonyl compounds. Active dicarbonyl compounds are further cross-linked with proteins to generate AGEs. Additionally, glucose autoxidation, Schiff base oxidative cleavage, Amadori product cleavage, and lipid peroxidation can all produce active dicarbonyl compounds, further generating AGEs. Song, Q.; Liu, J.; Dong, L.; Wang, X.; Zhang, X. Novel Advances in Inhibiting Advanced Glycation End Product Formation Using Natural Compounds. *Biomedicine & Pharmacotherapy* 2021.

During the Maillard reaction, Amadori product breaks down to generate some di-carbonyl compounds such as glyoxal (GO), methylglyoxal (MGO), and deoxyglucosones (3-DG) following both oxidative and nonoxidative pathways. These compounds are very reactive products, and they represent a critical step in AGEs generation because they can also generate hydroxyl aldehydes and the corresponding oxidized acid analogues [42]. For example, MGO can react with lysine residues generating the adducts, through a mechanism that involves intermediates like aldimine that can oxidize through a metal-catalyzed process giving deaminated allysine (adipic semialdehyde). This latter further oxidizes to yield 2-amino adipic acid, which indeed accumulates in oxidative-based disorders [43]. Several colorimetric and fluorimetric methods are available to determine parameters that are indicators of AGE production, such as the modification rate of lysine and arginine side chains, fructosamine content, aggregation state of the modified proteins, and AGE-specific fluorescence [44].

In addition to further rearrangements, reactive di-carbonyl compounds can lead to AGEs such as N^{ε} -carboxyethyllysine (CEL), arginine pyrimidine, pentosidine, pyrralin and N^{ε} -carboxymethyllysine (CML) [45].

In addition to endogenous AGEs formation, these compounds are also derived from foods and are called dietary AGEs (dAGEs). Usually, food high in lipids and proteins have the highest levels of dAGEs. Due to their harmful effect, dAGEs are also called glycotoxins [46]. Various processes such us thermal food processing, storage, frying and cooking can contribute to increase AGEs content causing oxidative stress and inflammation [47],[48].

AGEs act through different mechanisms, such as: crosslinking extracellular and intracellular proteins that imply alteration in the biochemical and physiological properties of proteins [49]; the binding to the cell surface receptor for AGEs (RAGE), which leads to the activation of intracellular signaling cascades causing the transcription of genes that have a central role in the pathogenesis of several diseases and the increase in the production of reactive oxygen species (ROS) [50].

Accumulation of AGEs has been found also in healthy aging persons, and it is worth noting that the accumulation of glycation adducts is involved in several diseases such as diabetes, renal diseases, and Alzheimer's disease [51] as well as in end stage renal disease, rheumatoid arthritis, sarcopenia and Parkinson's disease [52]. It has also been suggested that AGEs are involved in the loss of bone density and muscular mass associated with aging [53].

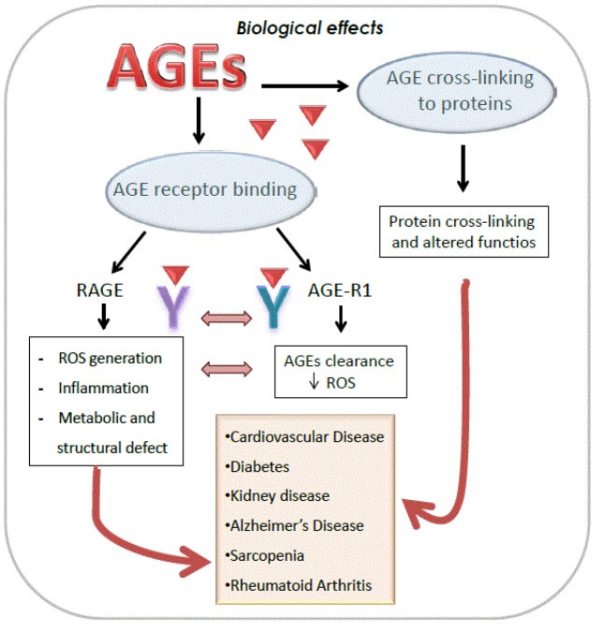

Figure 3. Biological effects of AGEs. Abate, G; Delbarba, A. Advanced Glycation End Products (Ages) in Food: Focusing on Mediterranean Pasta. *J Nutr Food Sci* 2015

2.2 Pathological effects of AGEs

The deleterious effects of AGEs in different tissues are attributed to their chemical, pro-oxidant, and inflammatory actions [54]. The biological effects of AGEs with RAGE involves the activation of the mitogen-activated protein kinases (MAPKs) and the phosphatidylinositol-3 kinase (PI3-K) pathways that will lead to the activation of the transcription factor NF-κB (nuclear factor kappa B). After activation, NF-κB translocates to the nucleus where it will activate the transcription of genes for cytokines, growth factors and adhesive molecules, such as tumor necrosis factor α (TNF-α), interleukin 6 (IL-6), well known inflammation promoters, and vascular cell adhesion molecule 1 (VCAM1) [55]. NF-κB activation increases RAGE expression, creating a positive feedback cycle that enhances the production of inflammation promoters. In addition, AGE-RAGE interaction activates NAD(P)H oxidase (a complex of enzymes which produces superoxide) and when this complex is upregulated, it increases intracellular oxidative stress [56].

ROS play a crucial role in the defense of pathogens, suggesting the protective effect of mild doses of oxidative stress but elevated levels of ROS lead to oxidation of proteins, lipids and nucleic acids increases [57]. Normally, there is a balance between oxidants and antioxidant defense. During aging, the equilibrium of prooxidants and antioxidants shifts to the former, leading to a marked rise in ROS. Usually, oxidized proteins are degraded by the 20S proteasome of the Ubiquitin–Proteasome-System (UPS) [58]. Due to their bulky structure, AGEs are able to block the entry of the proteasomal core

resulting in an increased in oxidized and damaged proteins. Further, elevated levels of oxidants promote the oxidation of lipids and glucose, resulting in the accelerated formation of AGEs [59].

In hyperglycaemia (HG) condition there is a mitochondrial dysfunction in endothelial cells and macrophages and aberrant activation of cytoplasmic NADPH oxidases (NOX) that together exacerbate ROS production that is associated with promotion of M1-like macrophage phenotype that favors the progression of diabetic complications [60].

Macrophages are innate immune cells with broad and dynamic phenotype plasticity, that quickly adapts to changes in microenvironmental cues. However, the traditional M1/M2 nomenclature is still utilized to reflect macrophage ability to exist in more pro-inflammatory (M1-like) or anti-inflammatory/immunosuppressive (M2-like) functional states [61]. For example, HG-activated endothelium recruits monocytes resulting in the release of pro-inflammatory cytokines and promotion of vascular damage. It is noteworthy that ROS production in diabetes is increased in both endothelial cells and monocytes/macrophages resulting in activation of pro-inflammatory pathways and reciprocal macrophage/endothelial cell interactions [62]. Another effect of HG is that glucose can chemically crosslink proteins, lipids and other molecules resulting in accelerated formation of AGEs. Endothelial cells and macrophages are the source of both AGEs and RAGE, thus the cross talk between these cell types is reciprocal. The engagement of AGEs and RAGE increase the production of ROS, especially hydrogen peroxide which serves as a mediator in pro-inflammatory response in endothelial cells and macrophages. As a result there is an increase in inflammatory response, oxidative stress and NF-κB activation [63].

2.3 AGEs and polyphenols

The inhibition of AGE formation by synthetic aminoguanidine (AMG) has been documented. However, the treatment with AMG in type 1 diabetics has caused serious complications [64]. The search for natural AGE inhibitors could thus represent a valid alternative approach. Indeed, the use of plant extracts showed to inhibit the AGE development more effectively than aminoguanidine. Therefore, phenolic compounds could represent a natural source of glycation inhibitors, being able to reduce the production of early Maillard reaction products [65],[66]. *In vivo* and *in vitro* studies also revealed positive effects of gallic acid on AGE-induced inflammation [67]. Antiglycative effects of different fruit and seed extracts have also been tested, suggesting that green pepper, peach, and promegranate have the highest capability to inhibit AGE formation [68].

Glycation inhibitors derived from natural compounds are good candidates for the development of new therapies against AGEs formation and other pathological conditions related to their accumulation such as diabetes and its complications [69].

Studies have shown some natural substances, such as resveratrol and curcumin, can prevent AGEs-induced pathology. Resveratrol inhibited the AGE-induced proliferation of collagen in smooth muscle cells of blood vessels [70] and curcumin blocked the effect of AGEs on the RAGE expression [71]. Park *et al*. evaluated the phenolic compound content of peanut extracts using various methods and in vitro experiments revealed that peanut extract not only inhibits the formation of AGEs but may also break glycated bonds [72].

Because of the diverse structures and functions of natural compounds, the mechanisms through which they inhibit AGE formation are also different: covering the glycation sites of proteins, scavenging oxidative free radicals, regulating AGE receptors, trapping active di-carbonyl compounds, chelating metal ions, inhibiting aldose reductase, and lowering blood glucose levels. The main mechanisms are reducing the levels of active carbonyl compounds and scavenging oxidative free radicals [41].

Some natural compounds bind competitively to proteins through hydrogen bonds or van der Waals forces, effectively protecting the structural integrity of the proteins and inhibiting nonenzymatic glycation. Indeed, AGEs can significantly modify protein structure altering their function [73]. Many natural compounds exhibit significant trapping of α-di-carbonyl compounds and inhibit AGE formation in a dose-dependent manner. For example, in phloretin, a glycoside, the 3-hydroxyl and 5-hydroxyl groups in its A ring are the main active centers that capture active di-carbonyl compounds. Phloretin forms specific adducts with MGO and GO, with scavenging rates of 80% and 68%, respectively, under normal metabolic conditions [74].

However, polyphenols have not yet been widely applied in clinical medicine because the first-pass effect in our bodies dramatically decreases the bioavailability of polyphenols through oxidation and glycosylation. Therefore, continued investigation of natural compounds and their specific mechanisms of action is necessary and will play a valuable role in inspiring drug discovery.

Chapter 3

3.1 GLUTs

The human glucose transporter (GLUTs) belongs to the Sugar Porter (SP) family, which as the largest branch of the Major Facilitator Superfamily (MFS). MFS proteins share a common fold comprising of 12 transmembrane helices (M1–M12) with a twofold pseudo-symmetry between the N-domain (M1-6) and the C-domain (M7-12). Due to the pseudo-symmetry, the A motif is found twice, located in the cytosolic loop connecting M2 and M3 of the N-domain and in the cytosolic loop connecting M8 and M9 of the C-domain. The importance of the SP motif has been demonstrated through mutational studies, and is highlighted by its strong conservation in the SP family. However, the functional role of the SP motif has not yet been established [75],[76]. SP proteins alternate their status exploring inward-facing and outward-facing conformations with respect to the central substrate binding site. When the transporter is in the outward-facing conformation (Cout), extracellular sugar can bind to the central binding site (CoutS), and be transported into the cell (CinS) as dictated by the concentration gradient across the membrane. The following conformational transition from the substrate-free inward conformation (Cin) to the substrate-free outward conformation (Cout) is needed to reset the transporter, and has been experimentally shown to be the rate-limiting step in GLUTs, consistent with thermodynamic model [77].

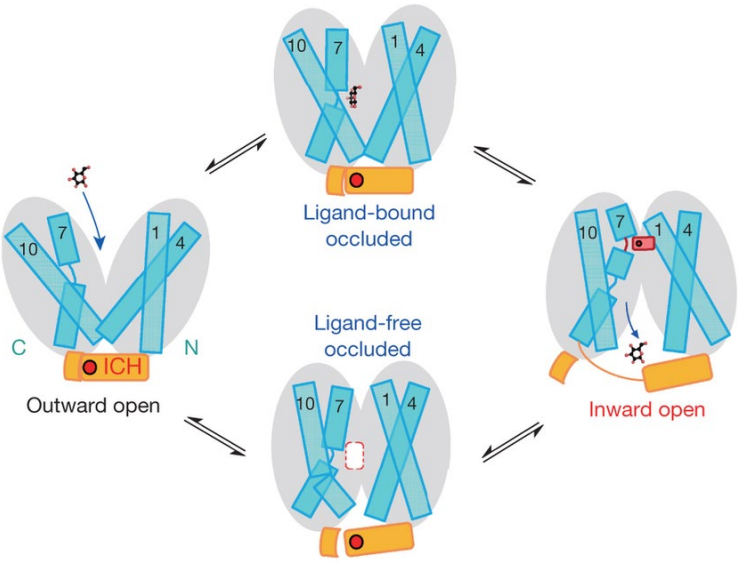

Figure 4. A working model for GLUT1: the different conformations between inward- and outward-facing conformations with respect to the central substrate-binding site and the transition between these two states define sugar transport. The ICH domain is illustrated as a closure in the intracellular gate in outward-facing conformations. The extracellular gate comprises some residues of TM1, TM4 and TM7 (red bricks in the 'open inward' illustration). Deng D, Xu C, Sun P, Wu J, Yan C, Hu M, Yan N. Crystal structure of the human glucose

transporter GLUT1. Nature. 2014 Jun 5;510(7503):121-5. doi: 10.1038/nature13306. Epub 2014 May 18. PMID: 24847886.

It is well established that residues of the A-motif stabilize GLUT proteins in an outward conformation, ready to receive glucose, via inter-TM salt bridges, and disruption of these networks triggers favorable formation of the inward state [78].

GLUTs proteins are primarily responsible for mediating cellular uptake of hexoses. However, the global biological importance of membrane transport proteins is reflected by their role in multiple aspects of cell biology and that membrane transporters represent between 5 and 15% of all coding genes in mammalian genomes. Therefore, expression and function of specific GLUT isoforms represent two important clinical/therapeutic variables and opportunities: as biomarkers, facilitating the prediction of clinical prognosis, staging and potential response to treatment; and as therapeutic targets for modulation (inhibition or activation) of their transport function. Diseases, including cancer and diabetes, are related to the dysfunction or mis-regulation of these transporters, identifying them as potential drug targets [79],[80].

The 14 GLUT isoforms present in humans show an amino acid identity of 19–65% (homology of 42–81%) but differ in substrate specificity, affinity, and tissue distribution. According to their sequence similarities, three classes of GLUTs have been defined with GLUT1-4 representing Class I, GLUTs 5, 7, 9, and 11 in Class II and GLUTs 6, 8, 10, 12, and 13 forming Class III [81].

GLUT1 is the most ubiquitously expressed GLUT isoform in human tissues. GLUT1 overexpression is reported in several tumor types, with the level of expression of GLUT1 associated with metastasis and poor patient survival [82]. GLUT1 is expressed in most human cells, often along with other class I glucose transporters. The GLUT1 transporter is present in high amounts in human erythrocytes [83].

GLUT2 localize primarily to the basolateral membrane of intestinal enterocytes, renal proximal tubular epithelium, and hepatocytes, with the probable function of glucose and fructose transport. GLUT2 is nevertheless required to equilibrate intracellular and extracellular glucose concentrations to ensure a proper control of glucose sensitive gene expression in the liver. In hepatocellular carcinoma (HCC), GLUT2 mRNA is expressed at higher levels than other GLUT isoforms, and GLUT2 expression shows a positive correlation with advanced clinical stage [84].

The biological function of the adult human brain requires high amounts of glucose, which is facilitated by the expression of GLUT3 in neurons and the cerebral cortex. Glioblastoma, the most common malignancy of the human brain was reported to express high levels of GLUT3 that was associated with poor patient survival [85].

GLUT4 is present mainly in the insulin-sensitive tissues of adipose, heart and skeletal muscle. Intracellular retention of GLUT4 in a specialized reservoir compartment is essential for maintaining a low rate of glucose transport in the basal state [86].

The features of class II GLUTs are the occurrence of the exofacial glycation site on the arginine in exofacial loop 5 (the linker between TM9 and TM10), with no glycation site on loop 1 as in class I and class III GLUTs. There seems to be preference for fructose rather than glucose as substrate. While, class III GLUT has the typical 12 TM spans. The asparagine N-linked glycation to asparagine occurs in loop 1. This class of GLUTs has intracellular targeting sequences, typically dileucine motifs, within the N-terminal domains. The presence of these sequences suggests at least some intracellular targeting and compartmentalized that may be related to function [87].

3.2 GLUTs-polyphenols interaction

The control of GLUT function is necessary for a regulated supply of metabolites (mainly glucose) to tissues. Pathophysiological abnormalities in GLUT proteins are responsible for, or associated with, clinical problems including type 2 diabetes and cancer and a range of tissue disorders, related to tissue-specific GLUT protein profiles. The availability of GLUT crystal structures has facilitated the search for inhibitors and substrates that are specific for each GLUT and that can be used for therapeutic purpose. The specificity and transport kinetic features of the GLUT proteins for hexose analogues and transport inhibitors have been most extensively studied for class 1 (GLUTs1-4) and for GLUT5 for defining differences between each of the GLUT proteins and ultimately for defining routes to the development of high affinity transport inhibitors [87].

Several compounds were discovered that effectively inhibit glucose uptake via GLUTs in cell lines. Flavonoids are known to have an inhibitory effect on GLUT2, including quercetin, phloretin, isoquercitrin and myricetin. However, most show little potency (IC50>60 μM), and the more potent inhibitors quercetin and phloretin (IC50 < 4 μM) inhibit not only GLUT2 but also other GLUTs. Identifying new, potent, and specific GLUT-2 inhibitors is desirable but challenging due to GLUT2 low affinity for glucose and fructose and a background uptake of these substrates by other GLUT isoforms in human cell lines [88],[89].

The consumption of tea flavonoids and other polyphenolic compounds are reported to have health benefits in individuals with or at risk of T2DM, for example, by improving glucose tolerance, enhancing insulin sensitivity, reducing oxidative stress and acting on glucose absorption in the proximal gut by inhibiting sugar transporters in the small intestine [90].

Chapter 4

Objectives

Numerous studies have attributed a wide range of biological activities to polyphenols, including anti-inflammatory, antioxidant and anti-cancer actions. Antiglycative effects have also been investigated. Several studies on natural compounds identified as waste products have showed their antioxidant activity in various tests, revealing that they could potentially be considered as an excellent source of natural antioxidants.

In our research, we characterized the possible properties of hazelnuts skin. Hazelnut represent an interesting source of by-products, producing a big amount of waste material with different polyphenols contents and molecular bio-diversity.

Accumulation of AGEs plays an important role in the pathogenesis of diabetic complications as well as in natural aging, renal failure, oxidative stress, and chronic inflammation.

Since AGEs contribute to the pathogenesis of several diseases, foods enriched or supplements containing natural bioactive molecules capable of inhibiting their production could represent an interesting new strategy to support therapeutic approaches with positive effect on human health.

The polyphenolic extract obtained by hazelnut skin has been characterized in qualitative and quantitative terms and its antioxidant activities was determined: polyphenols were extracted and characterized with HPLC-DAD/MS analysis. The concentration of total phenolic content obtained was quantified by Folin-Chocalteau method and then analyzed for evaluate their antioxidant activities with specific assay. Subsequently, we have product AGEs, reproducing the glycation reaction *in vitro*, considering several parameters such as the concentration of BSA and MGO (two component used for AGE production) and incubation time. Measurement of AGE-relative fluorescence gives an indication to AGEs formation.

To evaluate the anti-glycation activities of HSE, we have performed an *in vitro* analysis considering the capability of our extract compared to other compounds. Then, to assess the capability of HSE to prevent AGEs-derived damage, such us increased inflammation and ROS production, we chose THP-1 (human monocytes-derived macrophage) cellular model.

The formation of AGEs depending by the amount of glucose present in cells and tissues. In hyperglycemic condition, AGEs, both those that form endogenously as well as exogenous, contribute to the pathogenesis of obesity and diabetes. In humans, glucose transporter is facilitated by members of the glucose transporter family (GLUT, SLC2 gene family) and alterations in the functions or expression are involved in diabetes and cancer.

In silico approaches (molecular docking analysis) usually yield many compounds that need to be evaluated for their effect on hexose transport by GLUTs to select the best candidates for possible

(pre)clinical trials. Plant extract as polyphenols has been revealed a good candidate for the inhibition of GLUTs. We have performed, initially, *in silico* analysis with some compounds of HSE with GLUT1 and GLUT3, whose crystallographic structure are known. The interaction ligand-protein allowed as to evaluate the possible interaction between every single polyphenolic compound with these glucose transporters. Since the crystallographic structure of GLUT2 is not present, we propose to obtain it, in the future, following a more detailed study of the sequence based on the characteristics of GLUTs belonging to the same class and already characterized in this study.

GLUT2 plays an important role in maintaining glucose homeostasis in many human tissue like intestine, kidney and brain and for these reason GLUT2 is considered an important pharmaceutical target.

Chapter 5

Materials and methods

5.1 Preparation of HSE

Hazelnut skin was provided by Ferrero Hazelnut Company to evaluate the bioactive component and the possible use as nutraceutical following biological analysis.

The HSE was obtained following the procedure reported by Del Rio et al. [24] with some modifications. Two sequential extractions were applied: an amount of 0.5 g of hazelnut skins was added to 5 mL of 1% (v/v) aqueous formic acid solution in a 15 mL centrifuge tubes and was extracted for 30 min in an ultrasound bath (Elmasonic S30H, Elma Schmidbauer GmbH, Singen, Germany) at room temperature, frequency of 37 kHz, and heating power of 200W. Then, the sample was heated at 70 °C for 1 h and centrifuged for 10 min at 2151 g. The procedure was repeated two times, the supernatant was recovered and a second extraction was performed on the sample remaining after centrifugation. A solution of 5 mL of methanol/H_2O (75:25, v/v) was added and it was put for 15 min in an ultrasound bath (Elmasonic S30H, Elma Schmidbauer GmbH, Singen, Germany) and vortexed for 15 min. This procedure was repeated twice. After centrifugation, 10 min at 2151 g, the supernatant was recovered and added to the extract obtained with the first extraction step. The solvent of the total extract, was evaporated under vacuum at 30°C in a rotary evaporator (Eyela, Tokyo, Japan). The extract was then dissolved in 1 mL of MeOH and analyzed through HPLC-PDA/ESI-MS.

5.2 HPLC-PDA/ESI-MS analysis of HSE

HSE were analyzed using a Shimadzu Prominence LC-20A instrument (Shimadzu, Milan, Italy) equipped with two LC-20 AD XR pumps, SIL-10ADvp, CTO-20 AC column oven, and DGU-20 A3 degasser coupled to an SPD-M10Avp PDA detector and a mass spectrometer detector (LCMS-2010, Shimadzu, Tokyo, Japan) equipped with electrospray (ESI) interface. Separation was performed using a Core Shell column (150 µm,4.6 mm I.D., 2.7 µm d.p.) (Merck KGaA, Darmstadt, Germany), with the mobile phase composed by 1% aqueous formic acid (A) and acetonitrile (B), pumped at a flow rate of 1 mL/min. Phenolic compounds separation was obtained applying the following gradient: t = 00 0%B; t = 40 30%B; t = 41 100%B; t = 48 100%B; t = 49 0%B; t = 56 0%B. The injection volume was 2 µL. Data were acquired using a PDA in the range 210–400 nm and chromatograms were extracted at 360 nm and at 280 nm. MS-chromatograms were acquired in negative ionization mode, using the following parameters: nebulizing gas flow rate (N2): 1.5 mL min−1; event time: 1 s; mass spectral range: m/z100–800; scan speed: 1000 amu/s; detector voltage: 1.5 kV; interface

temperature: 250 ◦C; CDL temperature: 300 ◦C; heat block temperature: 300 ◦C; interface voltage: −3.50 kV; Q-array voltage: 0.0 V; Q-array RF: 150.0 V.

5.3 Determination of Total Phenolic Content

The total extract of hazelnut skin was dried as described above and resuspended in 5 ml of methanol/H_2O (50:50; v/v) solution, filtered with 0,22 µm filter in sterile conditions for use in cell cultures and subsequently analyzed for the total polyphenols content through a chemical reduction, measured by the Folin-Ciocalteau method [91]. Briefly, an aliquot of 20 µL of extract or standard compound was mixed with 100 µL of Folin reagent in 1580 µL of methanol/H2O (50:50; v/v) solution, followed by incubation for 8 min. Then, 300 µL of Na_2CO_3 0,2g/mL solution was added. The absorbance was measured after incubation at room temperature for 2 h, in the dark, using a microplate reader (Infinite 200 Pro, Tecan, Männedorf, Switzerland). The total phenolic content was determined from a standard curve using gallic acid (0−2000 µg/mL) as a standard and expressed as milligrams of gallic acid equivalents per grams of hazelnut fresh weight (mg GAE/g). All chemicals and reagents were purchased from Sigma (Sigma-Aldrich, Milan, Italy).

5.4 Determination of Antioxidant Activity

The antioxidant activity of hazelnut skin extract was determined by the TEAC and ORAC assays, according to a previously described method with some modification [92],[93]. The Trolox equivalent antioxidant capacity (TEAC) assay is based on the ability of the antioxidant present in a sample to scavenge the radical cation 2,20 -azino-bis (3-ethylbenzothiazoline-6-sulfonic acid) (ABTS) by spectrophotometric analysis. The radical cation $ABTS^{\cdot}$ was produced by reacting 7 mM ABTS with 2.5 mM potassium persulfate in aqueous phosphate buffer (5 mM, pH = 7,4) solution, stored in the dark at room temperature for 16 h. $ABTS^{\cdot+}$ is a blue-green chromogen with a characteristic absorption at 734 nm with an absorbance of 0.70 ± 0.04 [92]. Briefly, 10 µL of extract solution, gallic acid, or a standard compound were mixed with 190 µL of $ABTS^{\cdot+}$ solution diluted in phosphate buffer (5 mM, pH = 7.4) in a 96-multiwell plate. Antioxidant compounds in the reaction medium capture the free radical with a loss of color and therefore a reduction in absorbance, corresponding quantitatively to the concentration of antioxidants present. The absorbance was monitored after 10 min using a microplate reader (Infinite 200 Pro, Tecan, Männedorf, Switzerland). A calibration curve was prepared with Trolox as a standard (0–700 µM). Results were expressed as mmol Trolox equivalent (TE) per grams of hazelnut fresh weight or acid gallic.

Oxygen radical antioxidant capacity (ORAC) is another method used to estimate the total antioxidant capacity (TAC) of food or natural products based on the inhibition of the peroxyl-radical-

induced oxidation initiated by thermal decomposition of azo-compounds such as [2-20 -azo-bis(2-amidino-propane) dihydrochloride (AAPH)]. Fluorescein (FL) is used as the fluorescent probe. According to the method described previously [93], 50 µL of FL (78 nM) and 50 µL of sample, blank or standard were placed in a 96-multiwell-plate, which was heated to 37 ◦C for 15 min and then 25 µL of AAPH (221 mM) were added in each well. The fluorescence was measured immediately, and fluorescence intensity (excitation wavelength 485 nm and an emission wavelength of 535 nm) measurements were then taken every 5 min to 90 min using a microplate reader (Infinite 200 Pro, Tecan, Männedorf, Switzerland). A calibration curve was prepared with Trolox as a standard (0–50 µM). The ORAC values are expressed as mmol Trolox equivalents (TE) per grams of hazelnut fresh weight or acid gallic. All chemicals and reagents were purchased from Sigma (SigmaAldrich, Milan, Italy).

5.5 In Vitro Glycation Assay with BSA-MGO

AGE-BSA was prepared by reacting BSA with MGO according to the method described by Starowicz *et al.* with some modifications [94]. Briefly, BSA (100 mg/mL) and MGO (500 mM) were dissolved separately in PBS 1× (pH 7,4). Then, 2 mL of each sample were prepared by incubating BSA solution (4 mg/mL) with MGO solution at different concentrations (20-30-50-100 mM) in PBS 1× (pH 7.4) containing 0.02% NaN3 (to prevent microbe development) for 168 h at 37 ◦C, in the dark. Subsequently, BSA solution at different concentrations (2-4-10-25-50 mg/mL) with MGO (20 mM) were prepared in the same way. BSA solution without the addition of MGO was incubated under the same conditions and used as a control (BSA-non glycated).

Subsequently, to evaluate anty-glycation properties a solution of HSE, gallic acid or aminoguanidine at different concentrations (25–50–100–200– 400–500 µg/mL), was incubated in the dark with 4 mg/mL of BSA and 20 mM MGO (in phosphate buffer, pH 7.4, with 0.02% sodium azide). For each experimental condition, 2 mL of sample have been prepared and then incubated at 37 ◦C for 168 h. All chemicals and reagents were purchased from Sigma (Sigma-Aldrich, Milan, Italy).

After setting up the method to obtain AGEs, we choose one concentration of BSA and one concentration of MGO to prepare the AGEs to use in the cell line (THP-1 macrophages). We have used the same protocol described above with some modifications. Briefly, BSA (4 mg/mL) was dissolved in Phosphate buffer saline 1×, pH 7,4 (PBS, Corning, NY, USA) with the addition of 1% pen/strep (to prevent microbe development). BSA with or without addition of 20 mM MGO (BSA glycated and BSA-non-glycated respectively) were incubated for 168 h at 37°C, in the dark. All solution were filtered with 0,22 µm filter, in sterile conditions.

5.6 Measurement of AGE Fluorescence

The fluorescence of BSA-MGO model system (AGEs) was measured after incubation as described in detail previously using a microplate reader (Infinite 200 Pro, Tecan, Männedorf, Switzerland) at excitation/emission wavelengths 365/440 nm. Additionally, changes in intrinsic protein fluorescence were detected at excitation/emission wavelengths of 280/350 nm [44].

The inhibitory effect of treatment to gallic acid, aminoguanidine or hazelnut extracts was calculated using the following equation: [%] Inhibition = [1 − (fluorescence intensity of extract/fluorescence intensity of blank)] × 100.

Data are expressed considering IC50 concentrations, defined as the amount of extract or standard compound (µg/mL) required to reduce AGE formation by 50% and were determined by logarithmic regression analyses (n = 3) using GraphPad Prism software.

5.7 AGEs quantification

Quantification of the BSA-MGO or BSA samples was performed by BCA assay (Merck, Darmstadt, Germany) according to the protocol. Briefly for micro-scale assay were pipetted 25 µl each standard (BSA standard curve 0-25-125-250-500-1000 µg/ml) or sample replicate into individual wells of a 96-well plate. Then 200 µl BCA working reagent have been added to each well. For standard assay the plate was incubated at 37°C for 30 min. Subsequently the absorbance at 562 nm was measured in a microplate reader. To obtain the corrected absorbances, the absorbance of the blank standard was subtracted from the absorbance measurement or all other standard and protein samples. Using the standard curve, the absorbance of samples was interpolated within the linear range of the standard curve to obtain sample concentration.

5.8 Cell viability

Differentiated THP-1 macrophages (25.000 cells/well in 96-well plates) were exposed to different concentration of HSE (25-50-100-200-400-500 µg/mL GAE) and with BSA or BSA-MGO (100-150-300-450-600 µg/mL). Cells were treated with or without HSE for 1 h prior to BSA-MGO (300 µg/mL) treatment. Cytotoxicity was determined after 24 h of incubation by the MTT assay: cell culture medium was discarded, and each well was washed with 200 µL PBS. MTT solution 0.5 mg/mL (Sigma-Aldrich, Milan Italy), was added to cells (100 µL in each well) and the plate was incubated at 37° C + 5% CO_2 for 3 hours. Then MTT solution was removed, and 150 µL/well of dimethyl sulfoxide (DMSO, Sigma-Aldrich, Milan, Italy) was added to each well for dissolving the formazan crystals. Optical density (OD) was measured at 570 nm using a multifunctional microplate

reader (InfiniteM 200 Pro, TECAN, Männedorf, Switzerland). Cell viability was expressed as % of control (macrophages untreated).

5.9 ROS measurement

For measuring intracellular ROS, macrophages were used at density of 5x10^4 cells/well in 96-well black plates. Cells were loaded with 100 µL/well of H2DCF-DA (Merck, Darmstadt, Germany) diluted to 20 µM in PBS and incubated for 10 minutes at 37°C. Then the solution with probe was removed and replaced by 100 µL/well basal medium. Basic fluorescence intensity was measured at 495 nm excitation and 525 nm emission. Medium was removed and treatments were applied. After 60-minute fluorescence intensity was measured as described above [95].

5.10 Quantitative real-time PCR

Total RNA was isolated from cell by column-based method, Monarch Total RNA Miniprep Kit (New England BioLabs, Frankfurt am Main, Germany) according to manufacturer's instructions including DNAse I-treatment. Concentration and quality of isolated RNA was spectrophotometrically assessed by NanoDrop (Thermo Fisher Scientific Inc). Ready-to-use kit (Thermo Fisher Scientific, Waltham, Massachusetts, USA) was used to reverse transcription of 0.5 µg RNA, according to manufacturer's protocol. Quantitative real-time PCR was performed using SYBR green master mix (Applied Biosystems, Waltham, Massachusetts, USA). Primer sets for TNF-α (NM_000594.4; Fw: 5′-CTCCTCACCCACACCATCAGCCGCA-3′; Rv: 5′-ATAGATGGGCTCATACCAGGGCTTG-3′) and IL-1β (NM_000576.3; Fw: 5'-CTCGCCAGTGAAATGATGGCT-3'; Rv: 5'-TGGTGGTCGGAGATTCGTAGC-3'), were used. Actin-β (NM_001101.5; Fw: 5'-GGGAAATCGTGCGTGACATT-3'; Rv: 5'-TCGTAGATGGGCACAGTGT-3') was used as housekeeping gene to normalize data. All reactions were performed in triplicates. ΔΔCt method was used for data analysis. Values of genes of interest were first subtracted from the values of actin-β (ΔCt). N-fold change of gene expression was then calculated as 2^- (ΔCt treated-ΔCt untreated).

5.11 Cytokine quantification

The levels of human TNF-α and IL-1β were measured in the harvested supernatants by solid-phase sandwich Enzyme-Linked Immunosorbent Assay (ELISA kit; Thermo Fisher Scientific, Waltham, USA). THP-1 monocytes were seeded into six-well (1x10^6 cell/well) and differentiated into macrophages-M0. Cells were treated with 50 µg/mL HSE or 300 µg/mL BSA-MGO or in combination. After 24 h cell supernatant for each sample was collected and analysed according to the

manufacturer's recommendation. Optical density (OD) was measured using the microplate reader (InfiniteM 200 Pro, TECAN, Männedorf, Switzerland) at 450 nm.

5.12 Molecular modeling and docking analysis

To investigate the interaction between polyphenolic compounds in hazelnut skin and GLUTs we have performed in silico ligand screening. The structure of natural compounds tested were searched on PDB server [96]. The structure of GLUT1 in the inward-facing conformation (PDB ID: 5EQi) was used as experimental model. The structure of GLUT3 in the inward-facing conformation was obtained by homology modeling, using the crystal structure for GLUT1 inward-facing conformation (PDB ID: 6THA) as a template. We use the I-TASSER software [97] and excluded some templates such as all GLUT structures in outward-facing conformations. Two sites of interest for both GLUT1 and GLUT3, that represent the active sites of interaction of two specific inhibitors with receptors, were identified based on literature and verified for selected PDB files via the VMD software [98]. The docking prediction was performed with Haddock 2.4 software [99], [100]. Haddock returns, after a cluster analysis a series of models, to which a score is attributed to classify the model quality. The models with the highest Haddock score were selected for our analysis of receptor-ligand complex. We explicitly used Van der Waals energy and electrostatic energy as additional parameters to evaluate the interaction affinity for each model.

5.13 Statistical Analysis

The graphics and all statistical analysis were performed using GraphPad Prism version 5.0. The data were expressed as mean ± standard deviation of two/three independent experiments, with at least three technical replicates in each experiment. p-value, *$p < 0.05$, ** $p < 0.01$, *** $p < 0.001$ were considered statistically significant and was calculated using one-way ANOVA and Tukey as post-test or t-test of multiple or two comparisons, respectively. Different letters indicate a significative difference among samples.

Chapter 6

Results

6.1 HPLC-PDA/ESI-MS Quali-Quantitative Analysis of Phenolic Compounds in total Extracts of Hazelnut Skin

The HPLC-PDA/ESI-MS method, previously described, was applied for phenolic compounds determination in hazelnut skin. Qualitative analysis was performed considering the retention time, UV and MS spectra, use of standard compounds and data available in literature. Seventeen phenolic compounds have been identified in the extract. Twelve flavan-3-ols and two organic acids were detected at λ=280 nm while four flavonols and one dihydrochalcone were detected at λ=360 nm (Figure 5). All identified compounds, retention time and their mass-to-charge ratio (m/z) are summarized in Table 1. Gallic acid, protocatechuic acid, procyanidin B2 dimer, (-) epicatechin, epigallocatechin-gallate, myricetin rhamnoside, quercetin-3-rhamnoside, kampferol rhamnoside, myricetin, phloretin-2-o-glucoside, quercetin and kaempferol were identified based on retention time of standard molecules and the mass-to-charge ratio (m/z) of the molecular ion.

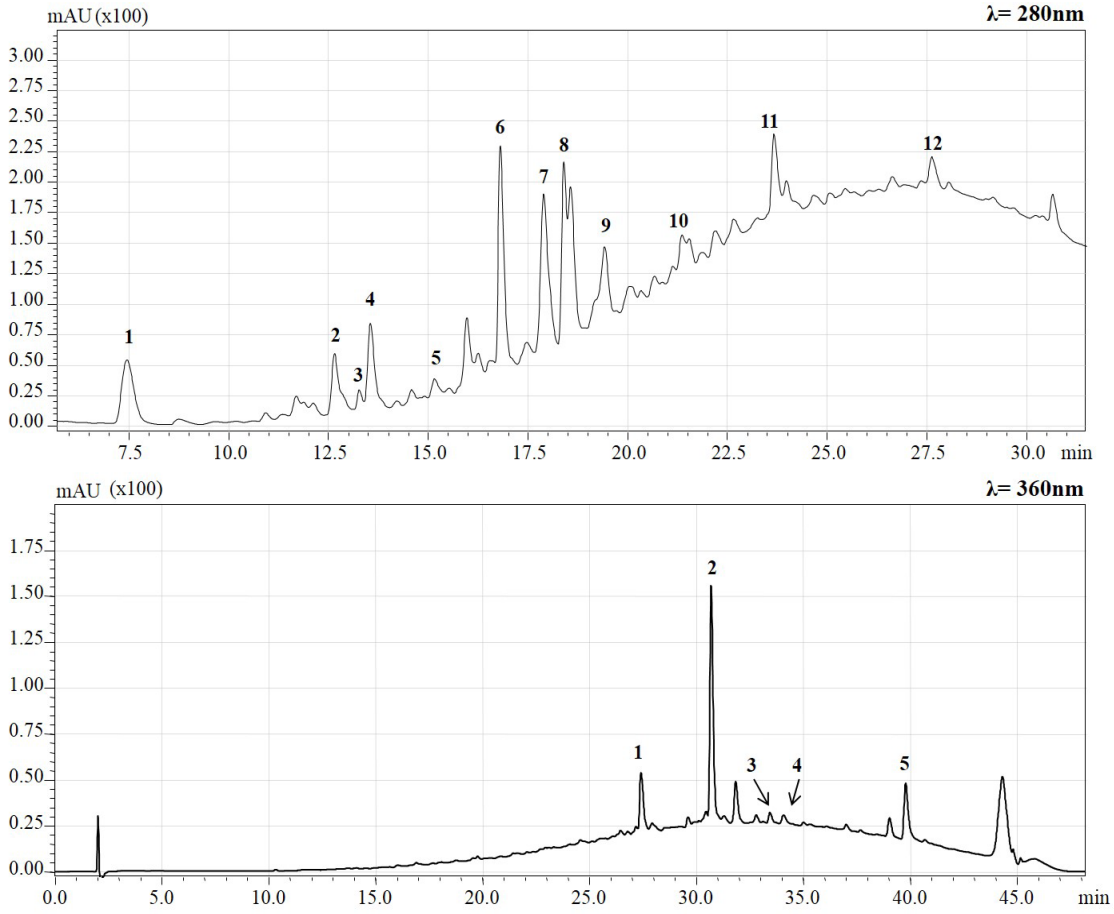

Figure 5. HPLC-PDA chromatograms, extracted at γ= 280nm and γ= 360nm, of hazelnut skin phenolic compound profile. Peak numbers refer to table 1.

For Procyanidin beta type dimer gallate, procyanidin C2 trimer, prodelphinidin B dimer and procyanidin dimers, molecular standards were not available and only mass-to-charge ratio (m/z) of the molecular ion was considered; (+) -catechin, and (-) -epicatechin, having the same mass-to charge ratio (m/z), were identified using purified (-) epicatechin as standard molecules and comparing the retention times. All the detected phenolic compounds were previously identified in hazelnut skin [24], [101]. Calibration curves with external standard were constructed for each available standard molecules and linearity concentration range was between 1 and 100 mg/L for each curve. Phenolic compounds were quantified using calibration curve of their standard molecule, if available, while procyanidins and prodelphinidins were quantified using the calibration curve of procyanidin B2 dimer, and (+) catechin using the calibration curve of (-) epicatechin. A total phenolic compounds concentration of 445 mg/100g was revealed. As previously reported by Del Rio *et al.* [24], flavan-3-ols represent the main class of phenolic compounds in hazelnut skin. Procyanidin dimers resulted to be the two compounds present in high quantity with a concentration of 100 and 93 mg/100g respectively, following by (+) catechin with a concentration of 62 mg/100g. Among detected flavonols, quercetin-3-rhamnoside showed the main quantity, with a concentration of 40 mg/100g, confirming data reported in literature [24]. Concentration of each identified phenolic compounds are reported in table 2.

N	Phenolic compound	tR	m/z $[M-H]^-$
Detected at λ=280 nm			
1	Gallic acid	7.4	169
2	Protocatechuic acid	12.6	153
3	Prodelphinidin B dimer	13.3	593
4	Procyanidin C2 trimer	13.5	865
5	Prodelphinidin B dimer	15.1	593
6	Procyanidin dimer	16.8	577
7	Procyanidin dimer	17.9	577
8	(+) Catechin	18.4	289
9	Procyanidin B2 dimer	19.4	577
10	(-) Epicatechin	21.3	289
11	Procyanidin beta type dimer gallate	23.7	729
12	Epicatechin gallate	27.6	441

Detected at λ=360 nm

1	Myricetin rhamnoside	27.3	463
2	Quercetin 3-rhamnoside	30.6	447
3	Kampferol rhamnoside	33.4	431
4	Phloretin-2-o-glucoside	34.9	435
5	Quercetin	39.7	301

Table 1. HPLC-PDA/ESI-MS identification of phenolic compounds in hazelnut skin extract.

Phenolic compounds	**Concentration mg (100 g)$^{-1}$ ± SD**
Gallic acid	15.683 ± 0.159
Protocatechuic acid	13.908 ± 1.440
Prodelphinidin B dimer	13.477 ± 0.000
Procyanidin C2 trimer	4.197 ± 0.058
Prodelphinidin B dimer	21.189 ± 0.400
Procyanidin dimer	100.480 ± 3.207
Procyanidin dimer	92.652 ± 1.115
(+) Catechin	62.137 ± 4.732
Procyanidin B2 dimer	15.552 ± 0.515
(-) Epicatechin	7.173 ± 0.000
Procyanidin beta type dimer gallate	16.803 ± 0.135
Epicatechin gallate	0.828 ± 0.099
Myricetin rhamnoside	16.465 ± 0.667
Quercetin-3-o-rhamnoside	39.623 ± 1.176
Kampferol rhamnoside	2.504 ± 0.048
Ploretin-2-o-glucoside	12.595 ± 0.568
Quercetin	10.658 ± 0.659
Total phenolic compounds	445.923 ± 7.312

Table 2. Phenolic compounds content in hazelnut skin extract

6.2 Total phenolic content and antioxidant capacity

Quantification of total phenolic content (TPC) in food or biological sample is based on the reaction of phenolic compounds with a colorimetric reagent which allows measurement in the visible spectrum. This approach is considered to give an approximation of the real polyphenol content. Total phenolic content (TPC) and antioxidant activities of hazelnut skin extract were determined by the

method previously described. Table 3 shows total phenolic compounds and the values of antioxidant power. Our results indicate that polyphenols in the skin represent about 70 mg GAE/g, (7 g of polyphenol/100 g of hazelnut skin) in line with literature data.

Compound	TPC (mg GAE/g)	TEAC (mmol TE/g)	ORAC (mmol TE/g)
HSE 100 mg/mL	70.07 ± 1.38	0.28 ± 0.03	0.35 ± 0.02
GA 1 mg/mL		10.98 ± 1.89	42 ± 3.34

Table 3. Total phenolic content (TPC) and antioxidant capacity (TEAC and ORAC). TPC of HSE expressed as mg of gallic acid per g of fresh weight. TEAC and ORAC expressed as mmol of trolox per g of fresh weight. All values are expressed as mean ± SD (n = 3). HSE, hazelnut skin polyphenolic extract; GA, gallic acid.

In relation to the antioxidant capability, it is worth noting that, although the antioxidant capability of skin extract was much lower than that of purified gallic acid (Table 3), no remarkable differences were evident between the two methods of analysis used. On the other hand, the antioxidant capability of gallic acid was about four times higher when measured by the ORAC assay than that observed by TEAC assay. Consequently, the difference in antioxidant capacity between HSE and purified gallic acid remarkably depend on the used methods. This is probably due to the presence in the skin extract of different molecules able to optimize the scavenging properties against the different oxidant species used in the two methods for the determination of antioxidant capacity. Meanwhile, when a purified molecule is used, different sensitivity/specificity in reacting with other chemical species could explain the remarkable difference in its antioxidant capacity.

6.3 AGEs quantification

Several methods are reported in the literature for measuring AGEs, many of which use the glycosylation of a standard protein by a standard glycosylation agent [16],[44],[102]. To evaluate whether AGEs formation was dependent on protein (BSA) or intermediate (MGO) concentration, different concentrations of MGO were incubated with BSA at a standard concentration (4 mg/mL). Figure 6 shows the formation of AGEs during 168 h of glycation reaction. The presence of total AGEs was characterized by fluorescence with respective excitation and maxima emission at 365 and 440 nm. The BSA-MGO model system shows a significant formation of fluorescent AGEs, which is already clear with the lowest MGO concentration uses (20 mM). As expected, in the control sample

(non-glycated BSA), a very low fluorescence was observed (Figure 6A). To confirm the MGO-dependent BSA glycation, the alterations in the fluorescence of BSA were analyzed: non-glycated BSA showed maximum fluorescence at 280/350 nm, while the 280/350 nm BSA fluorescence intensity strongly decreased as the consequence of MGO treatment (Figure 6B), thus confirming AGEs formation by inducing a conformational change in the protein [44].

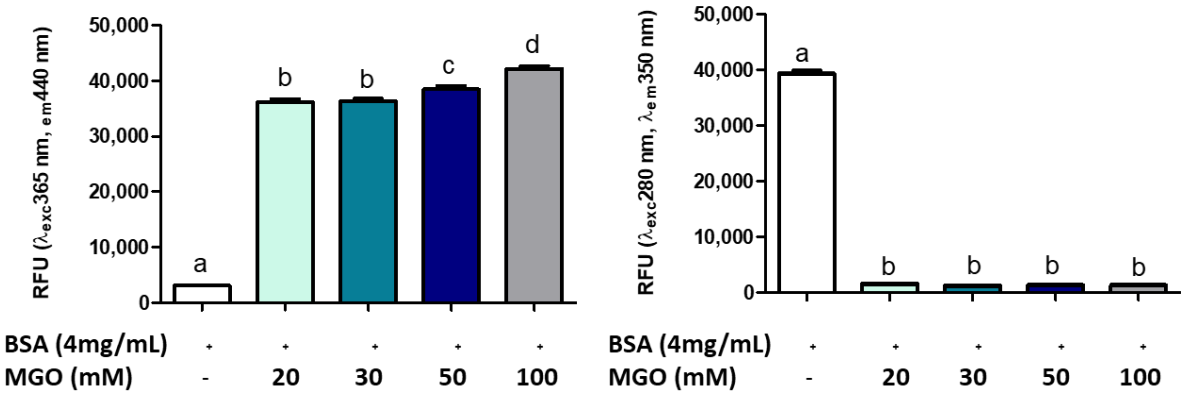

Figure 6. Fluorescence measurement of AGE after 168 h of incubation. All values are expressed as M ± SD (n = 3). Data represent relative fluorescence units (A) RFU λexc 365 nm/λem 440 nm and (B) RFU λexc 280 nm/λem 350 nm of BSA non-glycated (BSA) and BSA glycated (BSA+MGO). Different letters represent significant differences among sample (ANOVA one-way and Tukey post-test).

AGEs formation with dependence on protein concentration was also confirmed by using a range of 2–50 mg/mL BSA (Figure 7). The comparison between the amount of BSA and BSA-MGO complex at 365/440 nm and 280/350 nm indicates that, at 4 mg/mL, most of BSA was converted in the glycated form, while, at higher BSA concentrations, an increased amount of protein remained in the native form. Therefore, in the following set of experiments, 4 mg/mL BSA was used.

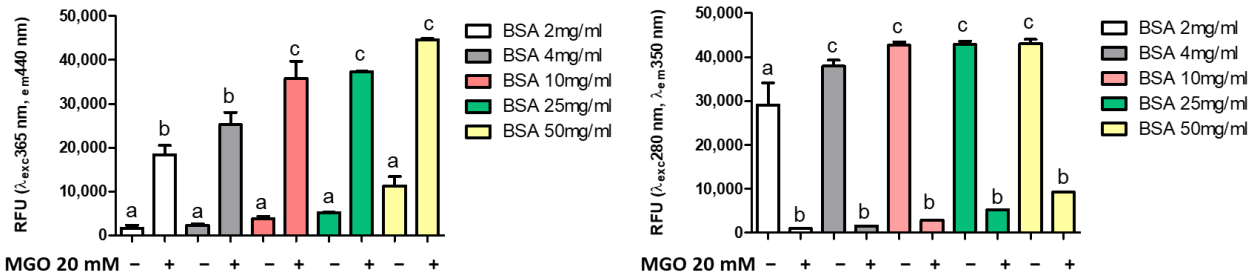

Figure 7. Fluorescence measurement of AGE after 168 h of incubation. All values are expressed as M ± SD (n = 3). Data represent relative fluorescence units (A) RFU λexc 365 nm/λem 440 nm and (B) RFU λexc 280 nm/λem 350 nm of BSA non-glycated (BSA) and BSA glycated (BSA+MGO). Different letters represent significant differences among sample (ANOVA one-way and Tukey post-test).

The comparisons of different fluorimetric analysis and timing suggests that, in our conditions (BSA 4mg/mL as standard protein and MGO 20 mM as glycosylated agent), the best time of incubation is seven days, since an incubation time over seven days did not determine a further increase in AGE formation (Figure 8). All fluorescent intensities were measured by a spectrophotometer (Infinite 200 Pro, Tecan, Männedorf, Switzerland).

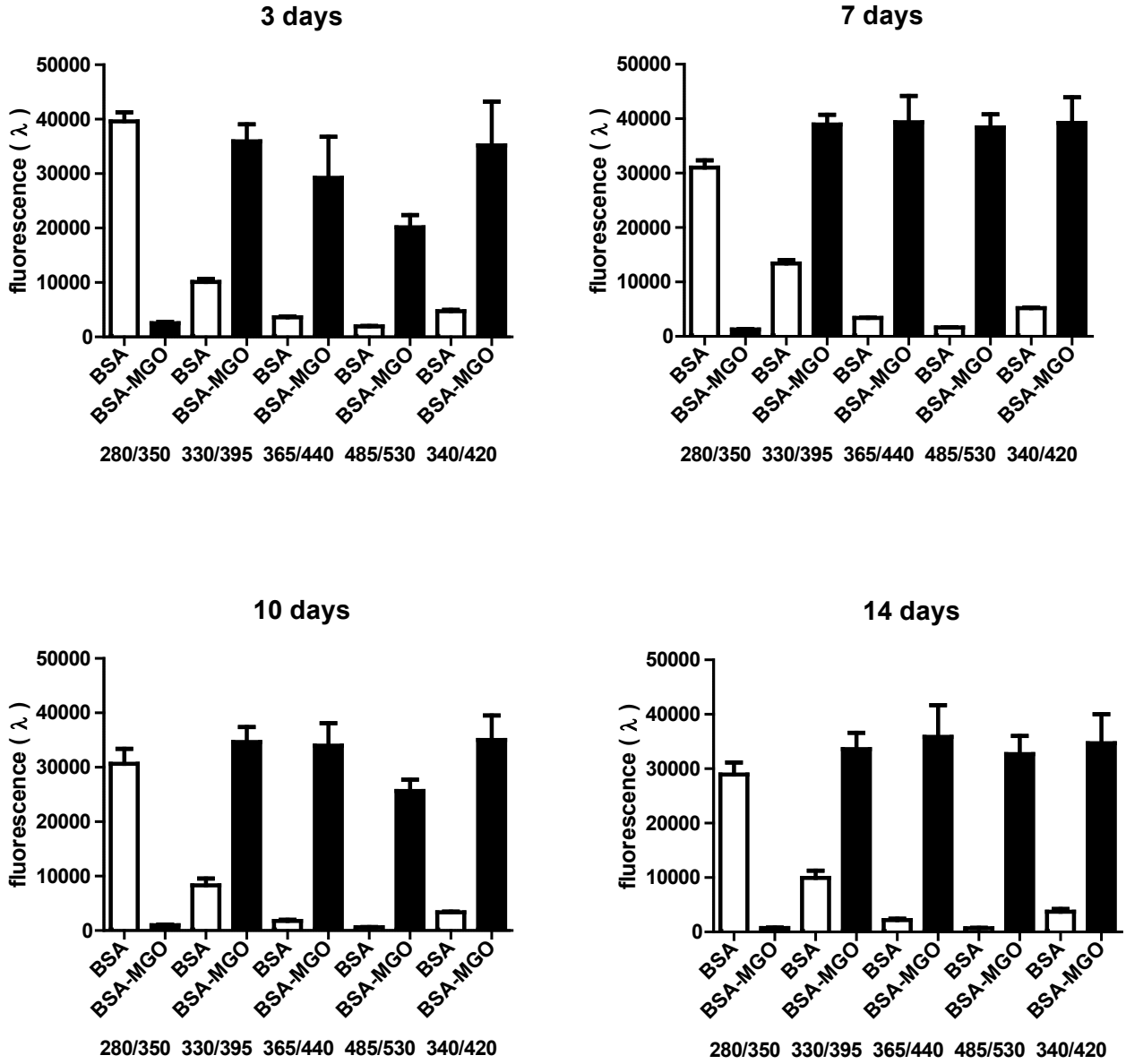

Figure 8. Comparison of Fluorescent AGE measurement at different time. The AGEs formation in dependence of BSA 4mg/ml incubated with 20 mM of MGO. All values are expressed as mean ± SD (*n* =3).

6.4 Inhibitory effect of hazelnut skin extract on AGEs

The capability of HSE to inhibit AGE formation was also investigated and compared with that of gallic acid, the efficiency of which inhibiting the in vitro AGE formation is known, in addition to that of AMG [102]. The effect of HSE on the inhibition of AGE formation was dose dependent (Figure 9). Interestingly, hazelnut skin capacity to inhibit AGE formation is slightly and much higher than that of aminoguanidine and gallic acid, respectively, as it is evident by their IC50 value (Table 4). The efficiency of a mix of bioactive molecules being higher than a single purified one has been reported for other molecules and biochemical/physio-pathological processes [103].

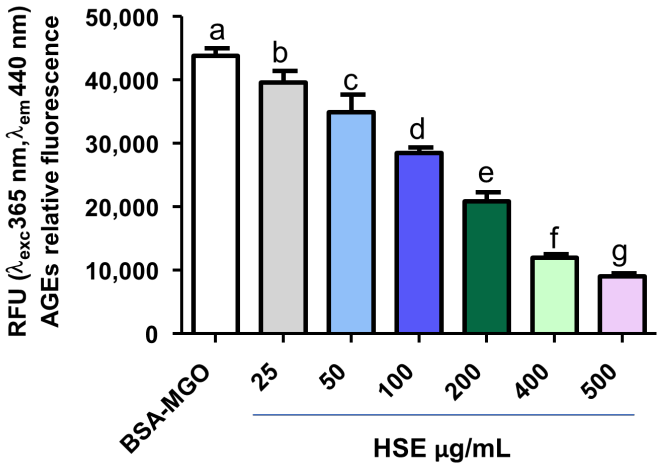

Figure 9. Inhibitory effect on AGE formation. Evaluation of HSE dose-response effect on AGE formation *in vitro*. BSA-MGO represents the control group. Different letters represent significant differences among sample (ANOVA one-way and Tukey post-test).

Compounds	IC50 (µg/ml)
HSE	109,7
GA	147,6
AMG	117,8

Table 4. IC50 value of synthetic or natural compounds: HSE (hazelnut skin polyphenolic extract), GA (gallic acid), and AMG (aminoguanidine). The concentration required for a 50% inhibition of the intensity of fluorescence (λ = 365/440 nm) was calculated from the dose–inhibition curve, obtained by GraphPad analysis (n = 3)

6.5 AGEs quantification for cell line treatment

In our work, we have used the BSA-MGO model for AGEs formation, as mentioned in materials and methods. The presence of total AGEs in the sample was characterized by fluorescence assay: the BSA-MGO sample shows a significant increase of specific AGE relative fluorescent unit at λex 365 nm/ λem 440 nm (figure 10A). On the contrary, non-glycated BSA showed maximum fluorescent at λex 280 nm/ λem 350 nm, as expected (figure 10B).

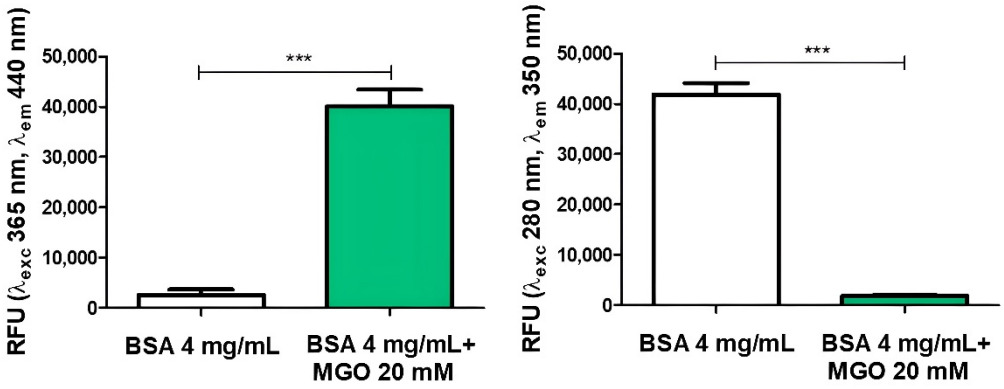

A B

Figure 10. Fluorescence measurement of AGEs after 168 h of incubation. Data represent relative fluorescence units (RFU) at A) λex 365 nm/λem 440 nm and B) λex 280 nm/λem 350 nm for BSA non-glycated (BSA) and BSA glycated (BSA+MGO). The analysis of variance was carried out using T-test analysis; ***$p<0.001$ value was considered significant (BSA vs BSA-MGO). All values are expressed as M ± SD (n = 3).

6.6 THP-1 derived macrophages

Monocyte-derived macrophages play a crucial role in inflammation, host defense, and tissue repair and have important pathogenic roles in many chronic diseases, such as asthma, inflammatory bowel disease, atherosclerosis, rheumatoid arthritis, and fibrosis [104],[105]. *In vivo*, human macrophages can be classified into two categories according to their activation states. A classical M1 phenotype driven by the cytokine interferon-(IFN-) γ and the activation of Toll-like receptors (TLRs) by lipopolysaccharide (LPS) and an alternative M2 phenotype triggered by interleukin IL-4, as well as IL-13 [106].

For our experiment we have chosen THP-1 cell line, monocyte isolated from peripheral blood from an acute monocytic leukemia patient. THP-1 was differentiated into macrophages and used for HSE or AGEs treatment to evaluate different biological aspects.

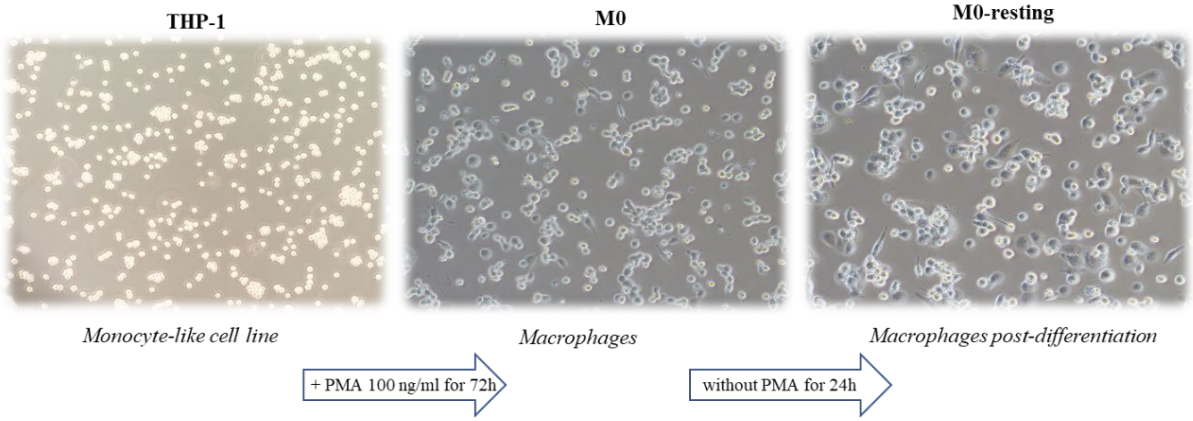

Figure 11. THP-1 cell line was differentiated into macrophages following PMA treatment for 72h. To obtain the resting state, cells were cultured for another day in medium without PMA and then used for the experiments.

6.7 Protective role of HSE on cell viability affected by AGEs

To assess whether the administration of the HSE could induce toxicity in a biological system, we performed cytotoxicity analysis. Macrophages were treated for 1 h with different concentration of HSE and then with BSA-MGO at 300 µg/mL for 24 h. MTT assay showed that HSE failed to display toxicity in macrophages up to the concentration of 400 µg/mL gallic acid equivalent (GAE) and only the administration of 500 µg/mL GAE was toxic (figure 12). This could explain why phenolic compounds lose their antioxidant capacity at high concentration and start to behave as prooxidants [107].

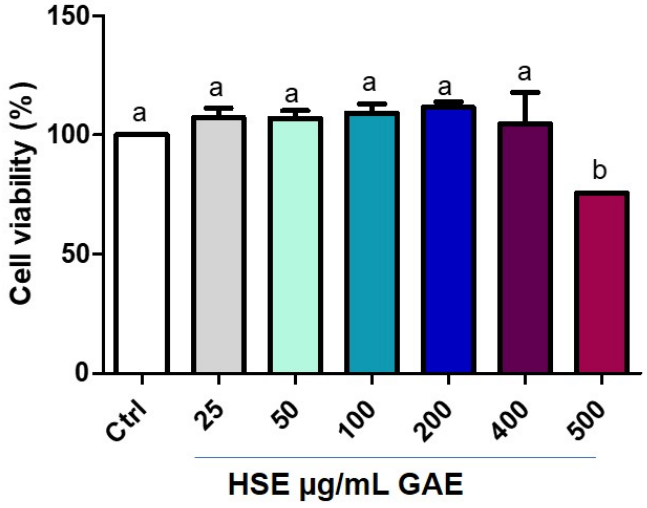

Figure 12. Cell viability after HSE treatment on THP-1 macrophages (M0). MTT assay was performed at 24 h post-treatment. Cell viability was expressed as % of control (non-treated). All data represent the means of at least 3 replicates ± standard deviation. The analysis of variance was carried out using the One-way ANOVA

test followed by the Tukey's Multiple Comparison Test One-way-Anova + Tukey's post-test: letters denote significant differences among sample.

On the contrary, BSA-MGO treatment resulted in the reduction of cell viability, in a dose-dependent manner (figure 13B), whereas administration of BSA alone did not significantly reduce macrophages viability (figure 13A).

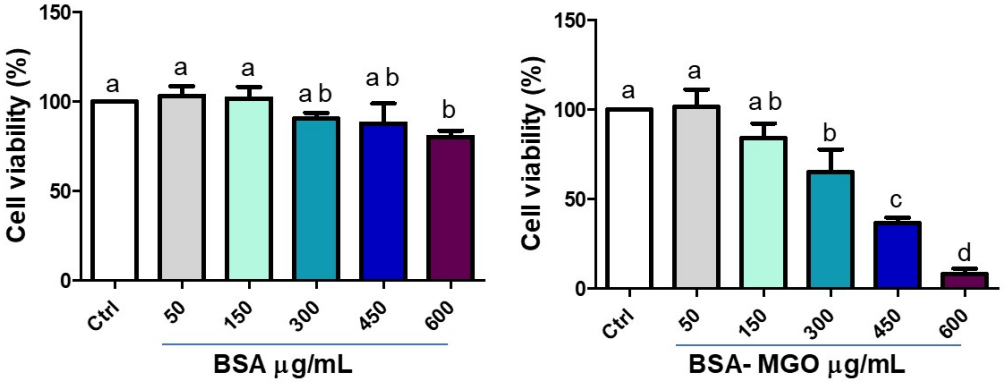

A B

Figure 13. Cell viability after A) BSA or B) BSA-MGO treatment on THP-1 macrophages (M0). MTT assay was performed at 24 h post-treatment. Cell viability was expressed as % of control (untreated). All data represent the means of at least 3 replicates ± standard deviation. The analysis of variance was carried out using the One-way ANOVA test followed by the Tukey's Multiple Comparison Test One-way-Anova + Tukey's post-test: letters denote significant differences among sample. (Ctrl vs 300 µg/ml BSA p=ns; Ctrl vs 300 µg/ml BSA-MGO **p<0.01).

In the co-treatment, HSE protects against the reduction in viability following BSA-MGO treatment (figure 14). Macrophages treated with BSA-MGO show a reduction in cell viability which increases following HSE treatment at low concentration. When using HSE at high concentrations (from 100 to 400 µg/mL GAE) seem to be a slight increase in viability but not significant compared to low concentration (50 µg/mL GAE).

In this contest, in order to evaluate ROS scavenging activity and the inhibition of inflammation induced by AGE (used at 300 µg/mL) the concentrations chosen for HSE was 50 µg/mL GAE.

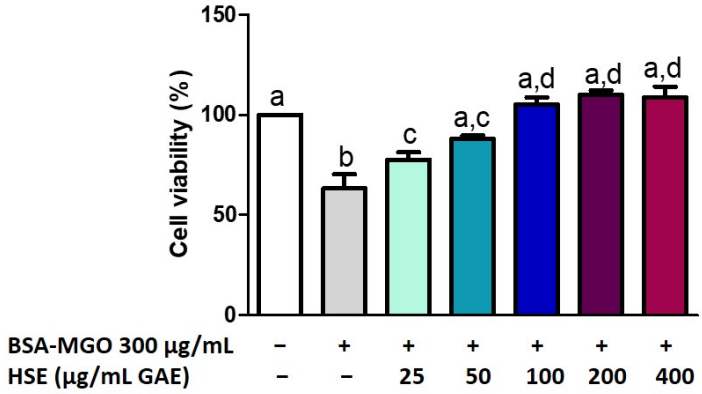

Figure 14. Cell viability after HSE co-treatment with BSA-MGO on THP-1 macrophages (M0). MTT assay was performed at 24 h post-treatment. Cell viability was expressed as % of control (non treated). All data represent the means of at least 3 replicates ± standard deviation. The analysis of variance was carried out using the One-way ANOVA test followed by the Tukey's Multiple Comparison Test One-way-Anova + Tukey's post-test: letters denote significant differences among sample.

6.8 Reduction of ROS by HSE

AGEs determine an increase in oxidative stress derived by different mechanism of actions [108]. Polyphenols have the ability to scavenge reactive carbonyl compounds and to donate an electron or hydrogen atom to free radicals [109]. Therefore, to evaluate if HSE exhibit protective effect against ROS, we have stimulated macrophages with AGEs and our results show that BSA-MGO leads to an increase in ROS production slightly higher than that observed in the control cell culture (Fig. 15). Interestingly, treatment with HSE remarkably inhibits ROS production increase. In addition, as shown in figure 15, the HSE at 50 µg/mL reduced ROS production induced by BSA-MGO (Mix).

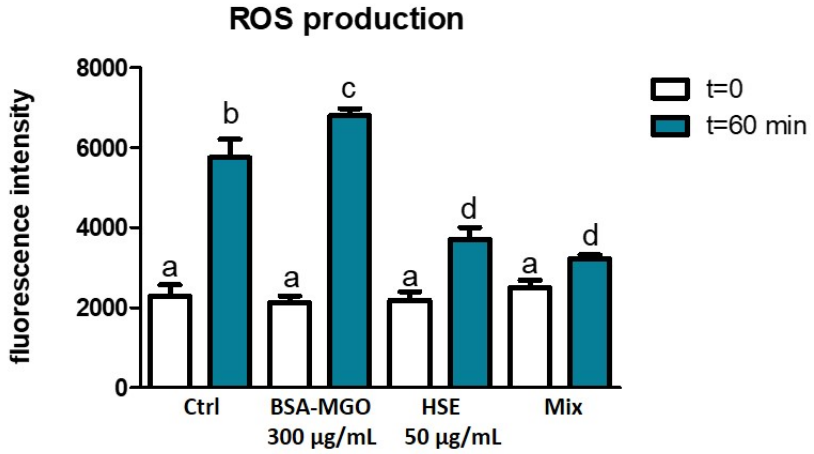

Figure 15. ROS production in macrophages. THP-1 macrophages M0 were treated with BSA-MGO, HSE or in combination (MIX) for up to 60 min. Production of intracellular ROS was determined using fluorescent probe H2-DCFDA and measurement of fluorescence intensity. Basic measurement (t=0) represents fluorescence intensity after loading with H2-DCFDA, without addition of any treatment. All data represent the

means of at least 3 replicates ± standard deviation. The analysis of variance was carried out using the One-way ANOVA test followed by the Tukey's Multiple Comparison Test: letters denote significant differences among sample (***p<0.001 BSA-MGO vs MIX, t=60 min).

6.9 Modulation of inflammatory gene expression by HSE

Inflammation plays a crucial role in the human body's defense against pathogens and other harmful stimuli. However, uncontrolled inflammation can trigger activated macrophages to secrete excessive inflammatory mediators, leading to damage of otherwise healthy tissue [110].

Here, we have demonstrated that BSA-MGO (our AGEs model system) leads to a slight but significant increase in mRNA expression for TNF-α gene expression, while co-treatment with BSA-MGO and HSE (Mix) has shown a reduction (figure 16A). BSA-MGO treatment have shown no effect on the IL-1β gene expression (figure 16B). Treatment of cell with LPS served as positive control for the pro-inflammatory cytokines gene expression (figure 16 A, B).

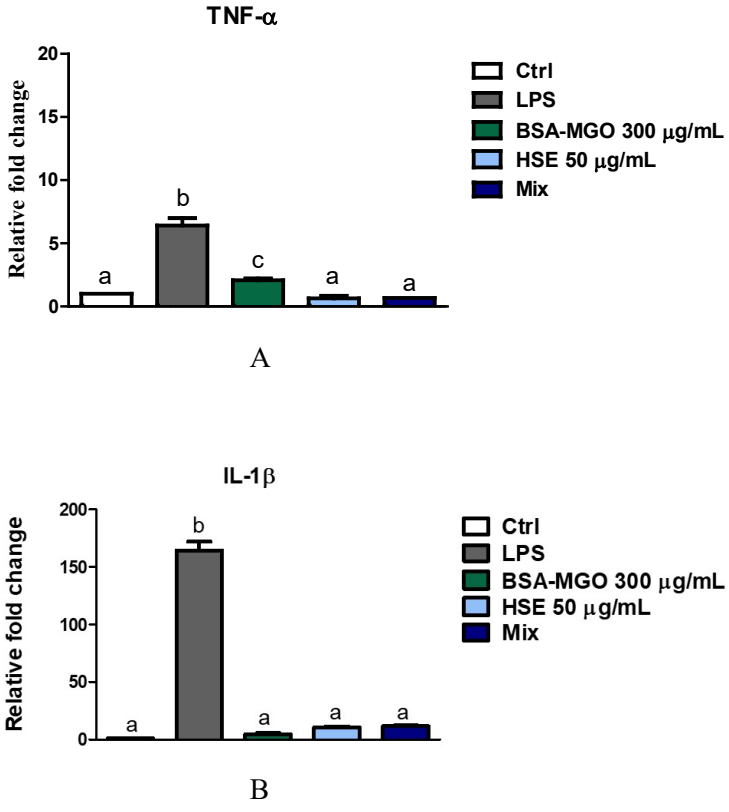

Figure 16. Expression of TNF-α and IL-1β**.** THP-1 macrophages (M0) were treated with BSA-MGO, HSE or in combination (MIX). Expression of A) TNF-α and B) IL-1β gene was quantified using qPCR after 24h. Data was normalized to untreated control cells. All data represent the means±SD of relative mRNA expression of 2 independent experiments. The analysis of variance was carried out using the One-way ANOVA test followed by the Tukey's Multiple Comparison Test: letters denote significant differences among sample. **p<0.01 BSA-MGO vs MIX for TNF-α; p=ns BSA-MGO vs MIX for IL-1 β).

6.10 Reduction of pro-inflammatory cytokines secretion

Production of pro-inflammatory cytokines TNF-α and IL-1β in THP1 cells was determined after 24 h treatment. Results showed that HSE attenuated macrophages inflammation caused by BSA-MGO stimulation for both TNF-α and IL-1β secreted protein levels after co-treatments of cells with BSA-MGO and polyphenolic extract (Mix) (figure 17 A, B).

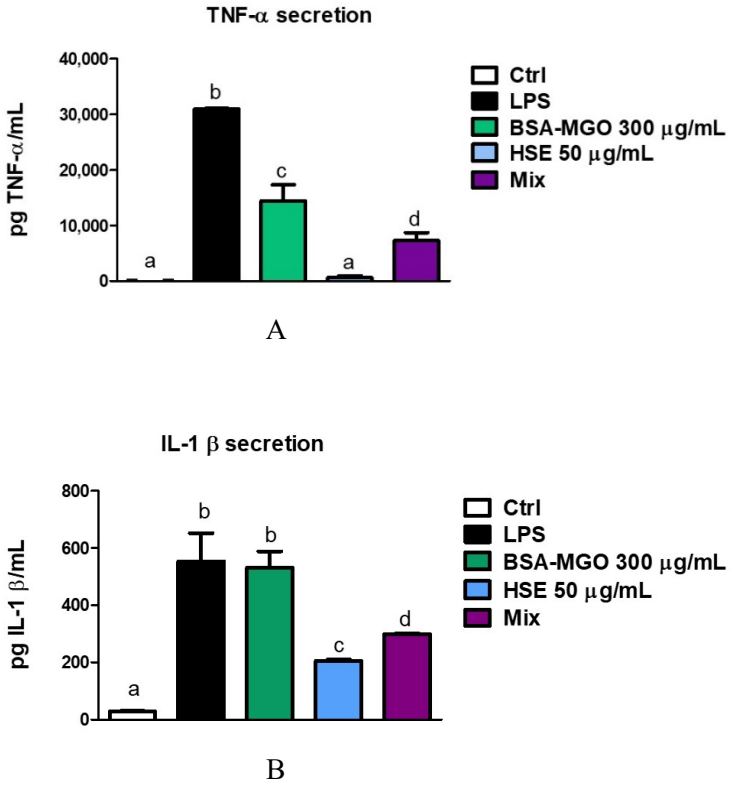

Figure 17. Quantification of pro-inflammatory cytokines TNF-α and IL-1β. THP-1 macrophages (M0) were treated with BSA-MGO, HSE or in combination (MIX). Levels of a) TNF-α and b) IL-1β secreted proteins was determined by ELISA assay, after 24h. Data were expressed as pg standard/ml. All data represent the means±SD of 2 independent experiments. The analysis of variance was carried out using the One-way ANOVA test followed by the Tukey's Multiple Comparison Test: letters denote significant differences among sample. **p<0.01 BSA-MGO vs MIX for TNF-α; *p<0.05 BSA-MGO vs MIX for IL-1 β).

6.11 In silico screening: protein-ligand interaction

Depending on which side of the cell membrane the substrate cavity opens to, GLUTs have two major conformations captured by the crystal structures of some isoforms and GLUT bacterial homologs. For Class I GLUTs, inward-facing conformations have been determined for GLUT1, and outward-facing conformations for GLUT3 [111].

The structural model of the GLUT1 open-inward facing conformation with cytocalasin B (PDB ID: 5EQi) represents our experimental model to study the possible interaction between GLUTs and some compounds present into our (poly)phenolic extracts, HSE. For the analysis, we chose four representative compounds such us epicatechin and catechin belonging to the flavan-3-ols, quercetin and gallic acid belonging to the flavonols and phenolic acid respectively.

Previous biochemical studies have shown that cytochalasin B inhibit GLUT1-mediated sugar transport by binding at or close to the GLUT1 sugar export site [112]. The virtual ligand screening by VMD software revealed the aminoacid interaction between GLUT1 and cytochalasin B, selected based on ligand-aminoacid distance (distance less lower than 3.5 angstroms). Protein-ligand interaction include SER80, TRP412, ANS411, THR137, PRO141, THR137, GLY384, TRP388, PHE291, PHE379, GLU380, PHE26, GLY408, HIS160, GLN161, ASN415, ILE287, GLN282, GLN283 (figure 18b). Two of these residues, TRP388 and GLY384 were used for molecular docking analysis for (poly)phenolic compounds of HSE. These residues were in common with glucose, that represent the substrate of GLUT1. The residues that characterized glucose-protein interaction were VAL165; GLN161; ASN317; TRP388; GLY384; GLN282; PHE379; GLU384 (figure 18a).

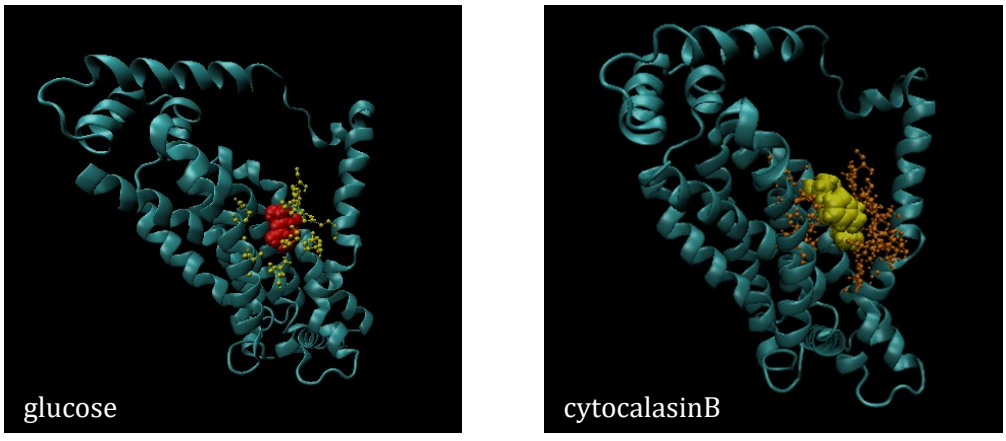

a b

Figure 18. Docking sites of glucose (a) and cytocalasinB (b) in the inward-open facing conformation GLUT1 (PDB ID: 5EQi) model. Ligand docks in the internal cavity. In figure A the glucose molecule (red) is represented with GLUT1 interacting aminoacids of interaction (yellow). In figure B the cytocalasin B (yellow)

and the corresponding aminoacid interaction (orange) are represented. To view the residues in the inner receptor pocket, some helices of the structure are not represented.

We modelled the interaction of other compounds with the receptor performing a docking calculation with HADDOCK2.4 software (as mentioned in materials and methods). We have specified two active sites, TRP388 and GLY384, to guide the haddock calculation. Comparing the Haddock scores we can rationalized that epicatechin, catechin and quercetin bind GLUT1 with higher affinity than glucose, while gallic acid has a lower affinity (figure 19). In table 4 we report the parameters used to quantify the ligand-binding interaction.

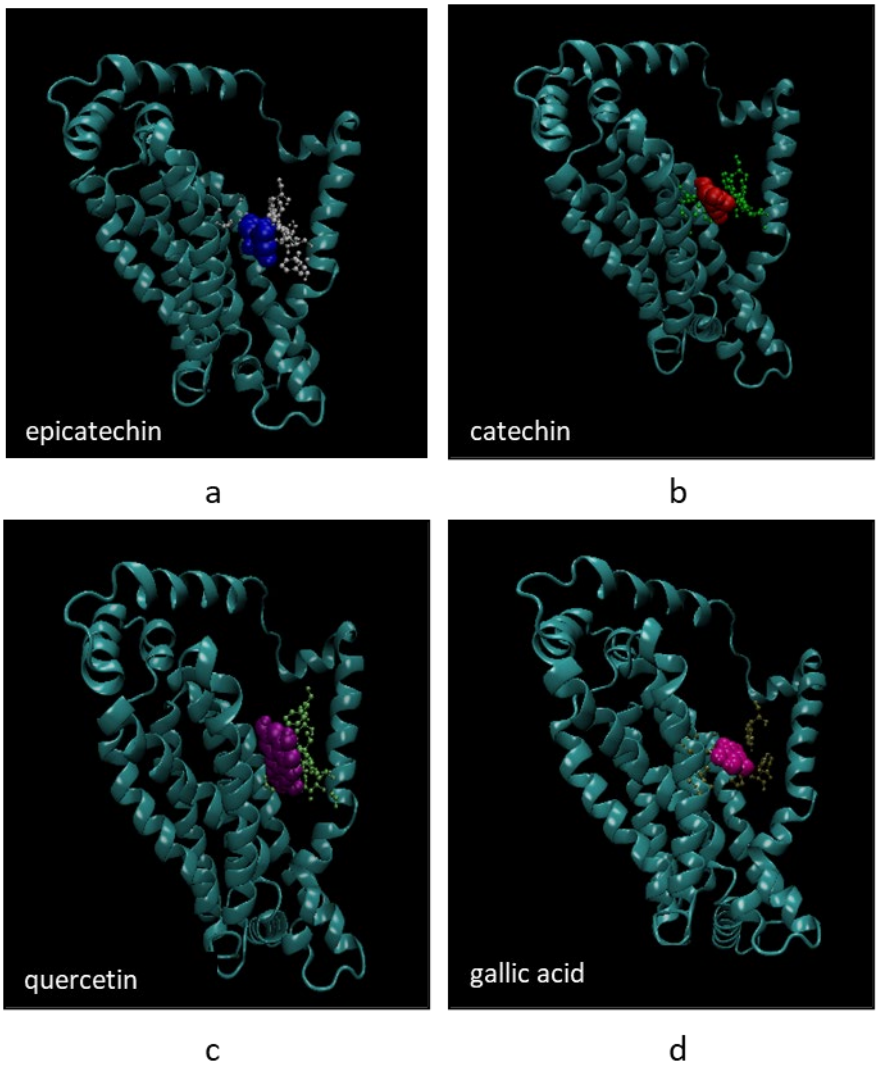

Figure 19. Docking sites of polyphenolic compounds with inward-open facing conformation GLUT1 (PDB 5EQi) model. Ligands dock in the internal cavity. a) epicatechin in blue, aminoacid in gray; b) catechin in red, aminoacid in green; c) quercetin in purple, aminoacid in light green; d) gallic acid in pink, aminoacid in brown.

	cytocalasinB	glucose	epicatechin	catechin	quercetin	gallic acid
Haddock score	-62.0 +/- 0.6	-26.4 +/- 0.8	-34.2 +/- 0.2	-34.2 +/- 0.6	-37.3 +/- 0.7	-22.6 +/- 1.2
Van der Waals energy	-36.9 +/- 1.3	-16.5 +/- 1.5	-24.9 +/- 2.4	-25.2 +/- 1.5	-27.2 +/- 1.6	-10.8 +/- 2.1
Electrostatic energy	-33.8 +/- 6.9	-43.1 +/- 13.5	-1.3 +/- 1.3	0.4 +/- 1.4	-10.8 +/-7.0	-42.0 +/- 10.3

Table 5. Data obstained by Haddock 2.4 software. Three quantities are reported sthat indicate the difference between different compounds when interacting with the receptor. The docking process was driven by specifying the active residues, TRP 388 and GLY 384.

The structural model for the GLUT3 inward-facing conformation (Figure 20) was modeled based on the crystal structure of GLUT1 (PDB ID: 6THa) with I-TASSER software.

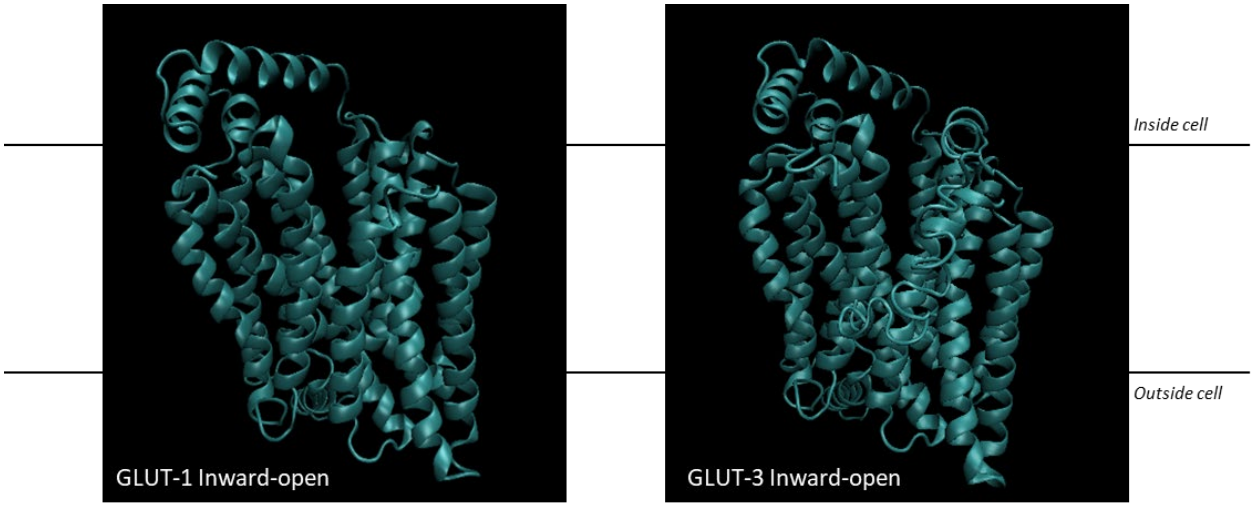

a b

Figure 20. a) Crystal structure of human sugar transporter GLUT1 in the inward conformation as template and b) crystal structure of GLUT-3 inward -open obtained.

We have tested the interaction between phenolic compounds and GLUT3. For these analysis we have choose two active sites, THR 135 and GLN280, based on literature [113]. As shown in figure 21 and in table 6 catechin, epicatechin and quercetin bind GLUT3 with higher affinity than glucose. Gallic acid binds with lower affinity compared to other molecules. The low affinity of gallic acid can be rationalized, in both cases, based on the small dimensions of the ligand with respect to the other considered molecules. Overall, all considered phenolic compounds present a good capacity to bind both receptors, relying on the same binding site of glucose. This docking investigation has to be considered a zero-level study of the interaction between ligand and receptor, as further modelling methods should be used to refine the results by including, for example, the explicit effect of the

solvent, and the kinetics and dynamics effects. Other important effects, as the role of concentration and the competition effects, cannot be easily modelled at present.

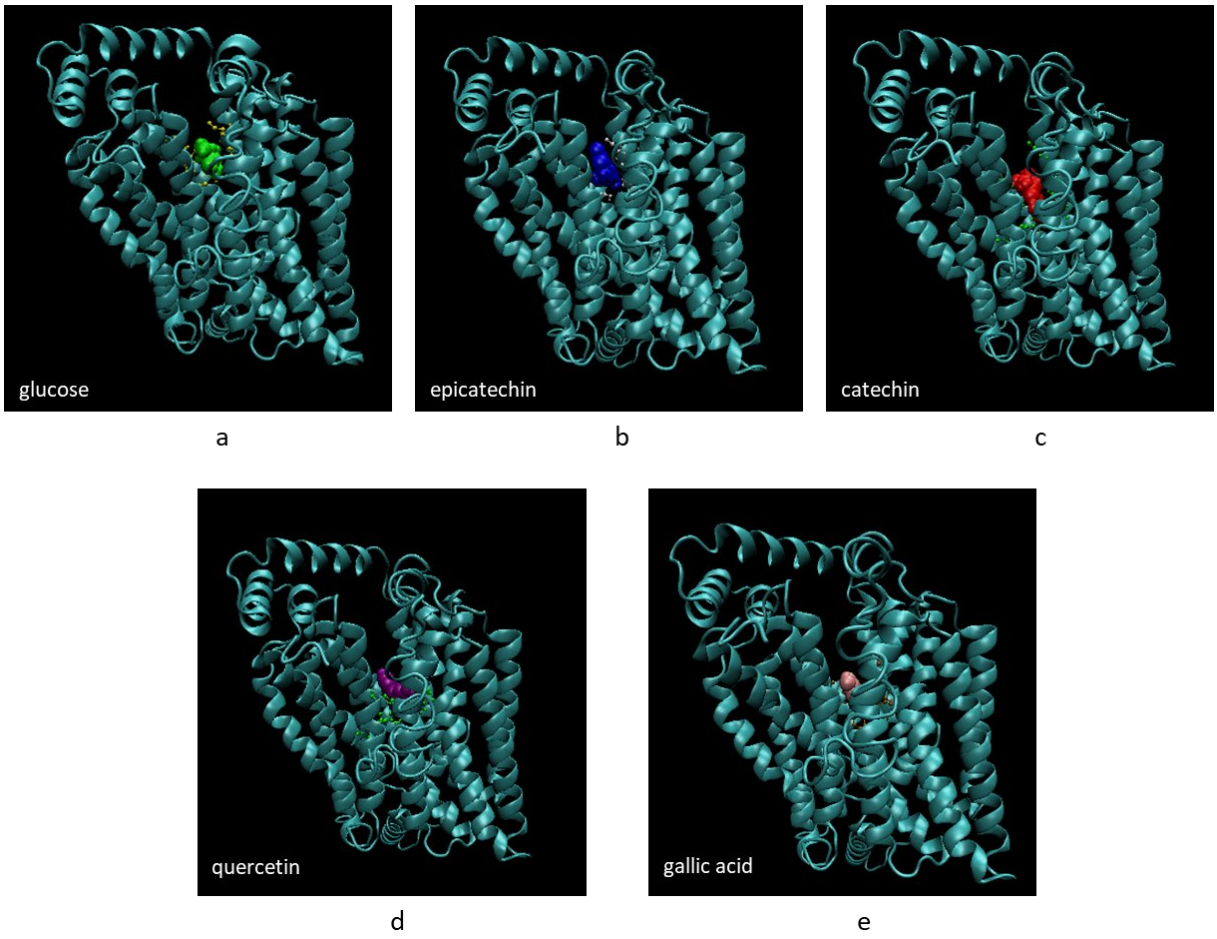

Figure 21. Docking sites of polyphenolic compounds with inward-open facing conformation GLUT3 (I-TASSER model). Ligands dock in the internal cavity. a) glucose in green; b) epicatechin in blue, c) catechin in red; d) quercetin in purple; e) gallic acid in pink.

	glucose	epicatechin	catechin	quercetin	Gallic acid
Haddock score	-22.9 +/- 0.3	-34.7 +/- 0.3	-35.1 +/- 0.1	-38.1 +/- 0.3	-24.7 +/- 0.3
Van der Waals energy	-20.2 +/- 0.3	-28.6 +/- 0.5	-27.8 +/- 0.3	-30.2 +/- 0.2	-17.0 +/- 0.3
Electrostatic energy	-8.9 +/- 2.6	0.5 +/- 0.6	2.7 +/- 1.2	-6.5 +/- 0.5	-26.2 +/- 1.4

Table 6. Analysis by haddock 2.4 software. We report three parameters that indicate the difference between different compound use for evaluate the possible interaction with receptor. The docking process was driven by specifying, as active residues, THR 135 and GLN 280.

Establishing the selectivity of GLUT inhibitors, particularly for class I, is crucial for future applications. Indeed, several GLUTs often coexist in the same tissue, and the ability to selectively modulate a single GLUT provides a powerful tool for unravelling its pathophysiological role. For GLUT2 the analysis presents some challenges, because the aminoacidic sequence of GLUT2 differs if compared with GLUT1 and GLUT3 (belonging to the same class), in the first 85 aminoacid. Furthermore, the GLUT2 isoform-2 differs from both GLUT2 and the other receptors, which made screening analysis more difficult. In figure 22 it is shown the initial part of the amino-acid sequence (aminoacids 1-84) of the GLUT2, GLUT2isoform2, GLUT3 and GLUT1 receptors. These and other differences in the sequence made us not possible, until now, to obtain a reliable homology model of GLUT2, using GLUT1 or GLUT3 as models. However, GLUT2 would represent an optimal model for performing polyphenol interaction analyses and it will deserve further investigations.

Figure 22. Align sequence of GLUT obtained with UniProt software:SP-P11168 GLUT2; SP-P11168-2 glut2 isoform2; NP_006507.2 GLUT3; NP-008862.1 GLUT1.

Chapter 7

Discussion

Diet is an important factor in preventing or modulating chronic and systemic inflammation and can influence normal physiology, whereas an unhealthy diet can have the opposite effect [114]. AGEs are a group of highly reactive chemical species and their accumulation contributes to hyperglycemia, metabolic burden, increase ROS production and inflammation which, along with insufficient production of endogenous antioxidants, induces oxidative stress leading to the development of chronic diseases [115],[116]. It is known that AGE accumulation in tissues is a natural consequence of aging, but it is accelerated in pathological conditions as well as in case of unhealthy diets where AGEs formation is enhanced by high-fructose diets [117].

During the last two decades, a large number of synthetic compounds have been tested for their inhibitory effect against AGEs formation but their use in clinical trials has been limited due to unwanted effect [118]. Plant-derived polyphenols have been shown to have glucose lowering activities and, in some cases, direct AGE inhibitory functions [119].

Recently, many studies have proposed the antiglycation activities by polyphenols based on different properties of polyphenol substances, including their structures, antioxidant abilities, and metabolism in the body. In literature is reported that (-)- epigallocatechin-3-gallate (EGCG), the major bioactive green tea polyphenol, efficiently traps reactive di-carbonyl compounds (MGO or GO) to form mono- and di-MGO or GO adducts under physiological conditions, reported to be less harmful. Also, EGCG was more reactive to trapping MGO than the pharmaceutical agent AMG [120]. Gallic acid (GA) showed a protective role in preventing AGE-mediated cardiac complications, through the attenuation of RAGE expression and also modulating inflammatory downstream signaling pathways [67].

The polyphenolic composition of hazelnut skins by HPLC-PDA/ESI-MS revealed that this food waste represents a rich source of several polyphenolic compounds. According to literature data, a mix of flavan-3-ols like procyanidins with their oligomerization forms, (+)-catechin and (−)-epicatechin is the main phenolic component in hazelnut skin (95%). Flavonols and dihydrochalcones represented an additional 3.5% while phenolic acids were responsible for less than 1% of the total identified phenolics in the HPLC-MS/MS method [24]. This confirms that hazelnut skin could be a relevant polyphenol source compared to the total phenol content (TPC) in hazelnut kernels that represent about 0.07–0.47 mg GAE/g [121].

In the last few years, accumulating evidence from epidemiological and clinical studies indicates that the daily intake of foods rich in polyphenols may possess protective effects in humans [5]. In this

context, a positive association between nut, including hazelnut, consumption, and lower risk of all-cause mortality and cardiovascular disease, has been observed [122],[123].

Hazelnut skin has been investigated as a functional ingredient rich of bio-active molecules, showing that its addition to coffee, bread, and yogurt improved their physiologically positive effects and antioxidative activity [124],[125]. The hazelnut skin extracts also revealed functional activity significantly improving the growth of two probiotic strains (Lactobacillus plantarum P17630 and Lactobacillus crispatus P17631), when added in bacterial media [126].

In vivo, hazelnut skin administration in hamsters improved their plasma lipid profile, following a high fat diet [127]. A recent report also shows a potential role for phenolic hazelnut skin extract as a UV protection booster [128].

It is known that antioxidant activity of polyphenols relies on their capability to give electrons or hydrogen ions to free radical molecules as well as to free radical scavenging compounds [129]. Moreover, polyphenols can also react with lysine and arginine residues, thus inhibiting the bond between MGO or GO, two major precursors of AGEs, and free aminoacids [130]. The capability of reducing AGE formation has been reported for several phenolic molecules, which are not present or present only as minor components in hazelnut skin [91]. Ferulic acid inhibited the advanced phase of the glycation [66]; epicatechin, p-coumaric acid, and gallic acid decreased protein carbonyls and AGE formation [102]; protocatechuic acid, dihydroferulic acid, p-coumaric acid, p-hydroxybenzoic acid and salicylic acid showed strong inhibition of AGEs formation, with better results in an oleic acid-BSA system than in a glucose-BSA system [16].

Other compounds like (-)-epigallocatechin-3- gallate (EGCG) and proanthocyanidins inhibited AGEs formation trapping MGO, with different flavonoids with vicinal dihydroxyl groups in the B-rings, such as myricetin, rhamnetin, quercetin, inhibiting fluorescence AGE development. Indeed, in the BSA-MGO system, quercetin traps MGO directly and then significantly inhibits the formation of AGEs [131],[132],[133].

Our data shows that HSE is able to counteract AGEs-induced damage *in vitro*. BSA-MGO (AGEs model system) in our study increased production of pro-inflammatory cytokines such as TNF-α and IL-1β in macrophages (M0) and HSE exert anti-inflammatory activity in particular against the expression of TNF-α. Instead, the protein secretion of both TNF-α and IL-1β was reduced significantly after administration of HSE. We have also demonstrated the antioxidant capacity of HSE, which reduced ROS production in macrophages stimulated by AGEs.

In light of this experimental evidence, we aim to further study in the next future the possible influence of HSE on AGE-RAGE signaling and on the activation of NF-κB pathway for a better understanding of the mechanism of action and the reduction of the inflammatory response caused by

AGEs, because these are correlated with the toxic effects linked with accumulation of AGEs that ultimately causes health complications [134].

Finally, we have investigated the relationship between polyphenols compounds of hazelnut skin and GLUTs transporter. Several flavonoids have inhibitory effect on GLUT2 like quercetin, phloretin, iso-quercetin and myricetin. These compounds inhibits also other GLUTs and for this reason the goal is identified specific GLUT inhibitors for understanding biological role in health and disease [135].

The protein-ligand interaction has been studied by *in silico* ligand screening. These computational approaches offer valuable alternative, opening the possibility to describe, at atomic level, physiologically relevant macromolecular complexes [136].

In our case we obtained those polyphenolic compounds such as catechin, epicatechin and quercetin bind with high affinity in the internal pocket both GLUT1 and GLUT3 transporter. Ligand interaction is driven by active residues, which represent interaction between GLUT and their inhibitor. Glucose, as expected, have low affinity with GLUT protein. Indeed, glucose moves into the cell by facilitated diffusion thought these transporters. Gallic acid has shown low binding affinity, probably due to the small size of the molecule compared to other compounds.

Use crystallographic structure of GLUT1 and GLUT3 we proposed to identified the crystal structure of GLUT2 to evaluate the interaction with polyphenol compounds to further studies.

The analysis of GLUT2 sequence revealed substantial difference in the first part of protein aminoacidic chain between GLUT of class I and probably these can explain the difficult in obtaining GLUT2 structure (with I-TASSER software) suitable for analysis.

Future studies will be conducted on the different conformations assumed by GLUTs, and in particular on the search for interactions between polyphenols and GLUT2, aiming to find molecules that can act as specific inhibitors.

References

1. Morand, C.; Tomás-Barberán, F.A. Contribution of Plant Food Bioactives in Promoting Health Effects of Plant Foods: Why Look at Interindividual Variability? *Eur J Nutr* **2019**, *58*, 13–19, doi:10.1007/s00394-019-02096-0.
2. Soare, A.; Khazrai, Y.M.; Fontana, L.; Del Toro, R.; Lazzaro, M.C.; Di Rosa, C.; Buldo, A.; Fioriti, E.; Maddaloni, E.; Angeletti, S.; et al. Treatment of Reactive Hypoglycemia with the Macrobiotic Ma-Pi 2 Diet as Assessed by Continuous Glucose Monitoring: The MAHYP Randomized Crossover Trial. *Metabolism* **2017**, *69*, 148–156, doi:10.1016/j.metabol.2017.01.023.
3. Ansari, M.Y.; Ahmad, N.; Haqqi, T.M. Oxidative Stress and Inflammation in Osteoarthritis Pathogenesis: Role of Polyphenols. *Biomed Pharmacother* **2020**, *129*, 110452, doi:10.1016/j.biopha.2020.110452.
4. Pandey, K.B.; Rizvi, S.I. Plant Polyphenols as Dietary Antioxidants in Human Health and Disease. *Oxid Med Cell Longev* **2009**, *2*, 270–278, doi:10.4161/oxim.2.5.9498.
5. Del Rio, D.; Rodriguez-Mateos, A.; Spencer, J.P.E.; Tognolini, M.; Borges, G.; Crozier, A. Dietary (Poly)Phenolics in Human Health: Structures, Bioavailability, and Evidence of Protective Effects against Chronic Diseases. *Antioxid Redox Signal* **2013**, *18*, 1818–1892, doi:10.1089/ars.2012.4581.
6. Cepas, V.; Collino, M.; Mayo, J.C.; Sainz, R.M. Redox Signaling and Advanced Glycation Endproducts (AGEs) in Diet-Related Diseases. *Antioxidants (Basel)* **2020**, *9*, 142, doi:10.3390/antiox9020142.
7. Mozaffarian, D. Dietary and Policy Priorities for Cardiovascular Disease, Diabetes, and Obesity: A Comprehensive Review. *Circulation* **2016**, *133*, 187–225, doi:10.1161/CIRCULATIONAHA.115.018585.
8. Doré, J.; Blottière, H. The Influence of Diet on the Gut Microbiota and Its Consequences for Health. *Current Opinion in Biotechnology* **2015**, *32*, 195–199, doi:10.1016/j.copbio.2015.01.002.
9. Han, X.; Shen, T.; Lou, H. Dietary Polyphenols and Their Biological Significance. *IJMS* **2007**, *8*, 950–988, doi:10.3390/i8090950.
10. Tsao, R. Chemistry and Biochemistry of Dietary Polyphenols. *Nutrients* **2010**, *2*, 1231–1246, doi:10.3390/nu2121231.
11. Adlercreutz, H.; Mazur, W. Phyto-Oestrogens and Western Diseases. *Annals of Medicine* **1997**, *29*, 95–120, doi:10.3109/07853899709113696.
12. Spencer, J.P.E.; Abd El Mohsen, M.M.; Minihane, A.-M.; Mathers, J.C. Biomarkers of the Intake of Dietary Polyphenols: Strengths, Limitations and Application in Nutrition Research. *Br J Nutr* **2008**, *99*, 12–22, doi:10.1017/S0007114507798938.
13. Selma, M.V.; Espín, J.C.; Tomás-Barberán, F.A. Interaction between Phenolics and Gut Microbiota: Role in Human Health. *J. Agric. Food Chem.* **2009**, *57*, 6485–6501, doi:10.1021/jf902107d.
14. Setchell, K.D.; Faughnan, M.S.; Avades, T.; Zimmer-Nechemias, L.; Brown, N.M.; Wolfe, B.E.; Brashear, W.T.; Desai, P.; Oldfield, M.F.; Botting, N.P.; et al. Comparing the Pharmacokinetics of Daidzein and Genistein with the Use of 13C-Labeled Tracers in Premenopausal Women. *The American Journal of Clinical Nutrition* **2003**, *77*, 411–419, doi:10.1093/ajcn/77.2.411.
15. D'Archivio, M.; Filesi, C.; Di Benedetto, R.; Gargiulo, R.; Giovannini, C.; Masella, R. Polyphenols, Dietary Sources and Bioavailability. *Ann Ist Super Sanita* **2007**, *43*, 348–361.
16. Chen, H.; Virk, M.S.; Chen, F. Phenolic Acids Inhibit the Formation of Advanced Glycation End Products in Food Simulation Systems Depending on Their Reducing Powers and Structures. *Int J Food Sci Nutr* **2016**, *67*, 400–411, doi:10.3109/09637486.2016.1166187.
17. Khan, M.; Liu, H.; Wang, J.; Sun, B. Inhibitory Effect of Phenolic Compounds and Plant Extracts on the Formation of Advance Glycation End Products: A Comprehensive Review. *Food Res Int* **2020**, *130*, 108933, doi:10.1016/j.foodres.2019.108933.
18. *Moving Forward on Food Loss and Waste Reduction*; FAO, Ed.; The state of food and agriculture; Food and Agriculture Organization of the United Nations: Rome, 2019; ISBN 978-92-5-131789-1.
19. Sagar, N.A.; Pareek, S.; Sharma, S.; Yahia, E.M.; Lobo, M.G. Fruit and Vegetable Waste: Bioactive Compounds, Their Extraction, and Possible Utilization. *Compr Rev Food Sci Food Saf* **2018**, *17*, 512–531, doi:10.1111/1541-4337.12330.
20. Martins, N.; Ferreira, I.C.F.R. Wastes and By-Products: Upcoming Sources of Carotenoids for Biotechnological Purposes and Health-Related Applications. *Trends in Food Science & Technology* **2017**, *62*, 33–48, doi:10.1016/j.tifs.2017.01.014.

21. Ran, X.-L.; Zhang, M.; Wang, Y.; Adhikari, B. Novel Technologies Applied for Recovery and Value Addition of High Value Compounds from Plant Byproducts: A Review. *Crit Rev Food Sci Nutr* **2019**, *59*, 450–461, doi:10.1080/10408398.2017.1377149.
22. Shahidi, F.; Alasalvar, C.; Liyana-Pathirana, C.M. Antioxidant Phytochemicals in Hazelnut Kernel (Corylus Avellana L.) and Hazelnut Byproducts. *J Agric Food Chem* **2007**, *55*, 1212–1220, doi:10.1021/jf062472o.
23. Pelvan, E.; Olgun, E.Ö.; Karadağ, A.; Alasalvar, C. Phenolic Profiles and Antioxidant Activity of Turkish Tombul Hazelnut Samples (Natural, Roasted, and Roasted Hazelnut Skin). *Food Chemistry* **2018**, *244*, 102–108, doi:10.1016/j.foodchem.2017.10.011.
24. Del Rio, D.; Calani, L.; Dall'Asta, M.; Brighenti, F. Polyphenolic Composition of Hazelnut Skin. *J Agric Food Chem* **2011**, *59*, 9935–9941, doi:10.1021/jf202449z.
25. Masullo, M.; Cerulli, A.; Mari, A.; de Souza Santos, C.C.; Pizza, C.; Piacente, S. LC-MS Profiling Highlights Hazelnut (Nocciola Di Giffoni PGI) Shells as a Byproduct Rich in Antioxidant Phenolics. *Food Res Int* **2017**, *101*, 180–187, doi:10.1016/j.foodres.2017.08.063.
26. Statista. Production of Tree Nuts Worldwide in 2019/2020, by Type (in 1,000 Metric Tons). Available Online: Https://Www.Statista.Com/Statistics/1030790/Tree-Nut-Global-Production-by-Type/ (Accessed on 19 August 2020).
27. Barbu, M.C.; Sepperer, T.; Tudor, E.M.; Petutschnigg, A. Walnut and Hazelnut Shells: Untapped Industrial Resources and Their Suitability in Lignocellulosic Composites. *Applied Sciences* **2020**, *10*, 6340, doi:10.3390/app10186340.
28. Alasalvar Cesarettin Antioxidant Activities and Phytochemicals in Hazelnut (Corylus Avellana L.) and Hazelnut By-Products. In.
29. Chaudhary, A.; Gustafson, D.; Mathys, A. Multi-Indicator Sustainability Assessment of Global Food Systems. *Nat Commun* **2018**, *9*, 848, doi:10.1038/s41467-018-03308-7.
30. DeFelice, S.L. The Nutraceutical Revolution: Its Impact on Food Industry R&D. *Trends in Food Science & Technology* **1995**, *6*, 59–61, doi:10.1016/S0924-2244(00)88944-X.
31. Shanmugam, M.; Kannaiyan, R.; Sethi, G. Targeting Cell Signaling and Apoptotic Pathways by Dietary Agents: Role in the Prevention and Treatment of Cancer. *Nutrition & Cancer* **2011**, *63*, 161–173, doi:10.1080/01635581.2011.523502.
32. Pacifico, S.; Piccolella, S.; Nocera, P.; Tranquillo, E.; Dal Poggetto, F.; Catauro, M. New Insights into Phenol and Polyphenol Composition of Stevia Rebaudiana Leaves. *Journal of Pharmaceutical and Biomedical Analysis* **2019**, *163*, 45–57, doi:10.1016/j.jpba.2018.09.046.
33. De Silva, S.F.; Alcorn, J. Flaxseed Lignans as Important Dietary Polyphenols for Cancer Prevention and Treatment: Chemistry, Pharmacokinetics, and Molecular Targets. *Pharmaceuticals* **2019**, *12*, 68, doi:10.3390/ph12020068.
34. Barbulova, A.; Colucci, G.; Apone, F. New Trends in Cosmetics: By-Products of Plant Origin and Their Potential Use as Cosmetic Active Ingredients. *Cosmetics* **2015**, *2*, 82–92, doi:10.3390/cosmetics2020082.
35. Sachdeva, V.; Roy, A.; Bharadvaja, N. Current Prospects of Nutraceuticals: A Review. *CPB* **2020**, *21*, 884–896, doi:10.2174/1389201021666200130113441.
36. Motawi, T.K.; Hamed, M.A.; Shabana, M.H.; Hashem, R.M.; Aboul Naser, A.F. Zingiber Officinale Acts as a Nutraceutical Agent against Liver Fibrosis. *Nutr Metab (Lond)* **2011**, *8*, 40, doi:10.1186/1743-7075-8-40.
37. Król, K.; Gantner, M. Morphological Traits and Chemical Composition of Hazelnut from Different Geographical Origins: A Review. *Agriculture* **2020**, *10*, 375, doi:10.3390/agriculture10090375.
38. Pycia, K.; Kapusta, I.; Jaworska, G. Changes in Antioxidant Activity, Profile, and Content of Polyphenols and Tocopherols in Common Hazel Seed (Corylus Avellana L.) Depending on Variety and Harvest Date. *Molecules* **2019**, *25*, 43, doi:10.3390/molecules25010043.
39. Luevano-Contreras, C.; Chapman-Novakofski, K. Dietary Advanced Glycation End Products and Aging. *Nutrients* **2010**, *2*, 1247–1265, doi:10.3390/nu2121247.
40. Hemmler, D.; Roullier-Gall, C.; Marshall, J.W.; Rychlik, M.; Taylor, A.J.; Schmitt-Kopplin, P. Evolution of Complex Maillard Chemical Reactions, Resolved in Time. *Sci Rep* **2017**, *7*, 3227, doi:10.1038/s41598-017-03691-z.

41. Song, Q.; Liu, J.; Dong, L.; Wang, X.; Zhang, X. Novel Advances in Inhibiting Advanced Glycation End Product Formation Using Natural Compounds. *Biomedicine & Pharmacotherapy* **2021**, *140*, 111750, doi:10.1016/j.biopha.2021.111750.
42. Vistoli, G.; De Maddis, D.; Cipak, A.; Zarkovic, N.; Carini, M.; Aldini, G. Advanced Glycoxidation and Lipoxidation End Products (AGEs and ALEs): An Overview of Their Mechanisms of Formation. *Free Radical Research* **2013**, *47*, 3–27, doi:10.3109/10715762.2013.815348.
43. Sell, D.R.; Strauch, C.M.; Shen, W.; Monnier, V.M. 2-Aminoadipic Acid Is a Marker of Protein Carbonyl Oxidation in the Aging Human Skin: Effects of Diabetes, Renal Failure and Sepsis. *Biochemical Journal* **2007**, *404*, 269–277, doi:10.1042/BJ20061645.
44. Schmitt, A.; Schmitt, J.; Münch, G.; Gasic-Milencovic, J. Characterization of Advanced Glycation End Products for Biochemical Studies: Side Chain Modifications and Fluorescence Characteristics. *Anal Biochem* **2005**, *338*, 201–215, doi:10.1016/j.ab.2004.12.003.
45. Valencia, J.V.; Weldon, S.C.; Quinn, D.; Kiers, G.H.; DeGroot, J.; TeKoppele, J.M.; Hughes, T.E. Advanced Glycation End Product Ligands for the Receptor for Advanced Glycation End Products: Biochemical Characterization and Formation Kinetics. *Analytical Biochemistry* **2004**, *324*, 68–78, doi:10.1016/j.ab.2003.09.013.
46. Sebeková, K.; Somoza, V. Dietary Advanced Glycation Endproducts (AGEs) and Their Health Effects--PRO. *Mol Nutr Food Res* **2007**, *51*, 1079–1084, doi:10.1002/mnfr.200700035.
47. Hellwig, M.; Henle, T. Baking, Ageing, Diabetes: A Short History of the Maillard Reaction. *Angew Chem Int Ed Engl* **2014**, *53*, 10316–10329, doi:10.1002/anie.201308808.
48. G, A.; A, D. Advanced Glycation End Products (Ages) in Food: Focusing on Mediterranean Pasta. *J Nutr Food Sci* **2015**, *05*, doi:10.4172/2155-9600.1000440.
49. Bidasee, K.R.; Zhang, Y.; Shao, C.H.; Wang, M.; Patel, K.P.; Dincer, Ü.D.; Besch, H.R. Diabetes Increases Formation of Advanced Glycation End Products on Sarco(Endo)Plasmic Reticulum Ca2+-ATPase. *Diabetes* **2004**, *53*, 463–473, doi:10.2337/diabetes.53.2.463.
50. Hegab, Z.; Gibbons, S.; Neyses, L.; Mamas, M.A. Role of Advanced Glycation End Products in Cardiovascular Disease. *World J Cardiol* **2012**, *4*, 90–102, doi:10.4330/wjc.v4.i4.90.
51. Chaudhuri, J.; Bains, Y.; Guha, S.; Kahn, A.; Hall, D.; Bose, N.; Gugliucci, A.; Kapahi, P. The Role of Advanced Glycation End Products in Aging and Metabolic Diseases: Bridging Association and Causality. *Cell Metabolism* **2018**, *28*, 337–352, doi:10.1016/j.cmet.2018.08.014.
52. Bengmark, S. Impact of Nutrition on Ageing and Disease. *Current Opinion in Clinical Nutrition & Metabolic Care* **2006**, *9*, 2–7, doi:10.1097/01.mco.0000171129.29278.26.
53. Odetti, P.; Rossi, S.; Monacelli, F.; Poggi, A.; Cirnigliaro, M.; Federici, M.; Federici, A. Advanced Glycation End Products and Bone Loss during Aging. *Annals of the New York Academy of Sciences* **2005**, *1043*, 710–717, doi:10.1196/annals.1333.082.
54. Ahmed, N. Advanced Glycation Endproducts—Role in Pathology of Diabetic Complications. *Diabetes Research and Clinical Practice* **2005**, *67*, 3–21, doi:10.1016/j.diabres.2004.09.004.
55. Lukic, I.K.; Humpert, P.M.; Nawroth, P.P.; Bierhaus, A. *The RAGE Pathway*. *Annals of the New York Academy of Sciences* **2008**, *1126*, 76–80, doi:10.1196/annals.1433.059.
56. Basta, G.; Lazzerini, G.; Del Turco, S.; Ratto, G.M.; Schmidt, A.M.; De Caterina, R. At Least 2 Distinct Pathways Generating Reactive Oxygen Species Mediate Vascular Cell Adhesion Molecule-1 Induction by Advanced Glycation End Products. *ATVB* **2005**, *25*, 1401–1407, doi:10.1161/01.ATV.0000167522.48370.5e.
57. Dupré-Crochet, S.; Erard, M.; Nüβe, O. ROS Production in Phagocytes: Why, When, and Where? *Journal of Leukocyte Biology* **2013**, *94*, 657–670, doi:10.1189/jlb.1012544.
58. Jung, T.; Catalgol, B.; Grune, T. The Proteasomal System. *Molecular Aspects of Medicine* **2009**, *30*, 191–296, doi:10.1016/j.mam.2009.04.001.
59. Ott, C.; Jacobs, K.; Haucke, E.; Navarrete Santos, A.; Grune, T.; Simm, A. Role of Advanced Glycation End Products in Cellular Signaling. *Redox Biol* **2014**, *2*, 411–429, doi:10.1016/j.redox.2013.12.016.
60. Kumar, P.; Swain, M.M.; Pal, A. Hyperglycemia-Induced Inflammation Caused down-Regulation of 8-OxoG-DNA Glycosylase Levels in Murine Macrophages Is Mediated by Oxidative-Nitrosative Stress-

Dependent Pathways. *The International Journal of Biochemistry & Cell Biology* **2016**, *73*, 82–98, doi:10.1016/j.biocel.2016.02.006.
61. Mantovani, A.; Biswas, S.K.; Galdiero, M.R.; Sica, A.; Locati, M. Macrophage Plasticity and Polarization in Tissue Repair and Remodelling: Macrophage Plasticity and Polarization in Tissue Repair and Remodelling. *J. Pathol.* **2013**, *229*, 176–185, doi:10.1002/path.4133.
62. Zheng, L.D.; Linarelli, L.E.; Liu, L.; Wall, S.S.; Greenawald, M.H.; Seidel, R.W.; Estabrooks, P.A.; Almeida, F.A.; Cheng, Z. Insulin Resistance Is Associated with Epigenetic and Genetic Regulation of Mitochondrial DNA in Obese Humans. *Clin Epigenet* **2015**, *7*, 60, doi:10.1186/s13148-015-0093-1.
63. Singh, V.P.; Bali, A.; Singh, N.; Jaggi, A.S. Advanced Glycation End Products and Diabetic Complications. *Korean J Physiol Pharmacol* **2014**, *18*, 1–14, doi:10.4196/kjpp.2014.18.1.1.
64. Thornalley, P.J. Use of Aminoguanidine (Pimagedine) to Prevent the Formation of Advanced Glycation Endproducts. *Archives of Biochemistry and Biophysics* **2003**, *419*, 31–40, doi:10.1016/j.abb.2003.08.013.
65. Liu, L.; Hedegaard, R.V.; Skibsted, L.H. Effect of Plant Polyphenols on the Formation of Advanced Glycation End Products from β-Lactoglobulin. *Food Sci Biotechnol* **2017**, *26*, 389–391, doi:10.1007/s10068-017-0053-y.
66. Silván, J.M.; Assar, S.H.; Srey, C.; Dolores del Castillo, M.; Ames, J.M. Control of the Maillard Reaction by Ferulic Acid. *Food Chemistry* **2011**, *128*, 208–213, doi:10.1016/j.foodchem.2011.03.047.
67. Umadevi, S.; Gopi, V.; Elangovan, V. Regulatory Mechanism of Gallic Acid against Advanced Glycation End Products Induced Cardiac Remodeling in Experimental Rats. *Chem Biol Interact* **2014**, *208*, 28–36, doi:10.1016/j.cbi.2013.11.013.
68. Mesías, M.; Navarro, M.; Gökmen, V.; Morales, F.J. Antiglycative Effect of Fruit and Vegetable Seed Extracts: Inhibition of AGE Formation and Carbonyl-Trapping Abilities. *J Sci Food Agric* **2013**, *93*, 2037–2044, doi:10.1002/jsfa.6012.
69. Perera, H.K.I.; Handuwalage, C.S. Analysis of Glycation Induced Protein Cross-Linking Inhibitory Effects of Some Antidiabetic Plants and Spices. *BMC Complement Altern Med* **2015**, *15*, 175, doi:10.1186/s12906-015-0689-1.
70. Mizutani, K.; Ikeda, K.; Yamori, Y. Resveratrol Inhibits AGEs-Induced Proliferation and Collagen Synthesis Activity in Vascular Smooth Muscle Cells from Stroke-Prone Spontaneously Hypertensive Rats. *Biochemical and Biophysical Research Communications* **2000**, *274*, 61–67, doi:10.1006/bbrc.2000.3097.
71. Tang, Y.; Chen, A. Curcumin Eliminates the Effect of Advanced Glycation End-Products (AGEs) on the Divergent Regulation of Gene Expression of Receptors of AGEs by Interrupting Leptin Signaling. *Lab Invest* **2014**, *94*, 503–516, doi:10.1038/labinvest.2014.42.
72. Park, S.; Do, M.; Lee, J.; Jeong, M.; Lim, O.; Kim, S. Inhibitory Effect of Arachis Hypogaea (Peanut) and Its Phenolics against Methylglyoxal-Derived Advanced Glycation End Product Toxicity. *Nutrients* **2017**, *9*, 1214, doi:10.3390/nu9111214.
73. Bhattacherjee, A.; Datta, A. Mechanism of Antiglycating Properties of Syringic and Chlorogenic Acids in in Vitro Glycation System. *Food Research International* **2015**, *77*, 540–548, doi:10.1016/j.foodres.2015.08.025.
74. Zhou, Q.; Gong, J.; Wang, M. Phloretin and Its Methylglyoxal Adduct: Implications against Advanced Glycation End Products-Induced Inflammation in Endothelial Cells. *Food and Chemical Toxicology* **2019**, *129*, 291–300, doi:10.1016/j.fct.2019.05.004.
75. Nomura, N.; Verdon, G.; Kang, H.J.; Shimamura, T.; Nomura, Y.; Sonoda, Y.; Hussien, S.A.; Qureshi, A.A.; Coincon, M.; Sato, Y.; et al. Structure and Mechanism of the Mammalian Fructose Transporter GLUT5. *Nature* **2015**, *526*, 397–401, doi:10.1038/nature14909.
76. Sun, L.; Zeng, X.; Yan, C.; Sun, X.; Gong, X.; Rao, Y.; Yan, N. Crystal Structure of a Bacterial Homologue of Glucose Transporters GLUT1–4. *Nature* **2012**, *490*, 361–366, doi:10.1038/nature11524.
77. Zhang, X.C.; Han, L. Uniporter Substrate Binding and Transport: Reformulating Mechanistic Questions. *Biophys Rep* **2016**, *2*, 45–54, doi:10.1007/s41048-016-0030-7.
78. Martens, C.; Shekhar, M.; Borysik, A.J.; Lau, A.M.; Reading, E.; Tajkhorshid, E.; Booth, P.J.; Politis, A. Direct Protein-Lipid Interactions Shape the Conformational Landscape of Secondary Transporters. *Nat Commun* **2018**, *9*, 4151, doi:10.1038/s41467-018-06704-1.

79. Ohtsubo, K.; Takamatsu, S.; Gao, C.; Korekane, H.; Kurosawa, T.M.; Taniguchi, N. N-Glycosylation Modulates the Membrane Sub-Domain Distribution and Activity of Glucose Transporter 2 in Pancreatic Beta Cells. *Biochemical and Biophysical Research Communications* **2013**, *434*, 346–351, doi:10.1016/j.bbrc.2013.03.076.
80. Barron, C.C.; Bilan, P.J.; Tsakiridis, T.; Tsiani, E. Facilitative Glucose Transporters: Implications for Cancer Detection, Prognosis and Treatment. *Metabolism* **2016**, *65*, 124–139, doi:10.1016/j.metabol.2015.10.007.
81. Mueckler, M.; Thorens, B. The SLC2 (GLUT) Family of Membrane Transporters. *Molecular Aspects of Medicine* **2013**, *34*, 121–138, doi:10.1016/j.mam.2012.07.001.
82. Mergenthaler, P.; Lindauer, U.; Dienel, G.A.; Meisel, A. Sugar for the Brain: The Role of Glucose in Physiological and Pathological Brain Function. *Trends in Neurosciences* **2013**, *36*, 587–597, doi:10.1016/j.tins.2013.07.001.
83. Cura, A.J.; Carruthers, A. Role of Monosaccharide Transport Proteins in Carbohydrate Assimilation, Distribution, Metabolism, and Homeostasis. In *Comprehensive Physiology*; Terjung, R., Ed.; Wiley, 2012; pp. 863–914 ISBN 978-0-470-65071-4.
84. Thorens, B. GLUT2, Glucose Sensing and Glucose Homeostasis. *Diabetologia* **2015**, *58*, 221–232, doi:10.1007/s00125-014-3451-1.
85. Cosset, É.; Ilmjärv, S.; Dutoit, V.; Elliott, K.; von Schalscha, T.; Camargo, M.F.; Reiss, A.; Moroishi, T.; Seguin, L.; Gomez, G.; et al. Glut3 Addiction Is a Druggable Vulnerability for a Molecularly Defined Subpopulation of Glioblastoma. *Cancer Cell* **2017**, *32*, 856-868.e5, doi:10.1016/j.ccell.2017.10.016.
86. James, D.E.; Strube, M.; Muecdler, M. Molecular Cloning and Characterization of an Insulin-Regulatable Glucose Transporter. *Nature* **1989**, *338*, 83–87, doi:10.1038/338083a0.
87. Holman, G.D. Structure, Function and Regulation of Mammalian Glucose Transporters of the SLC2 Family. *Pflugers Arch - Eur J Physiol* **2020**, *472*, 1155–1175, doi:10.1007/s00424-020-02411-3.
88. Kwon, O.; Eck, P.; Chen, S.; Corpe, C.P.; Lee, J.; Kruhlak, M.; Levine, M. Inhibition of the Intestinal Glucose Transporter GLUT2 by Flavonoids. *FASEB j.* **2007**, *21*, 366–377, doi:10.1096/fj.06-6620com.
89. Schmidl, S.; Tamayo Rojas, S.A.; Iancu, C.V.; Choe, J.-Y.; Oreb, M. Functional Expression of the Human Glucose Transporters GLUT2 and GLUT3 in Yeast Offers Novel Screening Systems for GLUT-Targeting Drugs. *Front. Mol. Biosci.* **2021**, *7*, 598419, doi:10.3389/fmolb.2020.598419.
90. Ni, D.; Ai, Z.; Munoz-Sandoval, D.; Suresh, R.; Ellis, P.R.; Yuqiong, C.; Sharp, P.A.; Butterworth, P.J.; Yu, Z.; Corpe, C.P. Inhibition of the Facilitative Sugar Transporters (GLUTs) by Tea Extracts and Catechins. *The FASEB Journal* **2020**, *34*, 9995–10010, doi:10.1096/fj.202000057RR.
91. Fanali, C.; Tripodo, G.; Russo, M.; Della Posta, S.; Pasqualetti, V.; De Gara, L. Effect of Solvent on the Extraction of Phenolic Compounds and Antioxidant Capacity of Hazelnut Kernel. *ELECTROPHORESIS* **2018**, *39*, 1683–1691, doi:10.1002/elps.201800014.
92. Ellouze, I.; Abderrabba, M.; Sabaou, N.; Mathieu, F.; Lebrihi, A.; Bouajila, J. Season's Variation Impact on *Citrus Aurantium* Leaves Essential Oil: Chemical Composition and Biological Activities. *Journal of Food Science* **2012**, *77*, T173–T180, doi:10.1111/j.1750-3841.2012.02846.x.
93. Huang, D.; Ou, B.; Hampsch-Woodill, M.; Flanagan, J.A.; Deemer, E.K. Development and Validation of Oxygen Radical Absorbance Capacity Assay for Lipophilic Antioxidants Using Randomly Methylated β-Cyclodextrin as the Solubility Enhancer. *J. Agric. Food Chem.* **2002**, *50*, 1815–1821, doi:10.1021/jf0113732.
94. Starowicz, M.; Zieliński, H. Inhibition of Advanced Glycation End-Product Formation by High Antioxidant-Leveled Spices Commonly Used in European Cuisine. *Antioxidants (Basel)* **2019**, *8*, 100, doi:10.3390/antiox8040100.
95. Bezold, V.; Rosenstock, P.; Scheffler, J.; Geyer, H.; Horstkorte, R.; Bork, K. Glycation of Macrophages Induces Expression of Pro-Inflammatory Cytokines and Reduces Phagocytic Efficiency. *Aging (Albany NY)* **2019**, *11*, 5258–5275, doi:10.18632/aging.102123.
96. Fermi, G.; Perutz, M.F.; Shaanan, B.; Fourme, R. The Crystal Structure of Human Deoxyhaemoglobin at 1.74 Å Resolution. *Journal of Molecular Biology* **1984**, *175*, 159–174, doi:10.1016/0022-2836(84)90472-8.

97. Yang, J.; Yan, R.; Roy, A.; Xu, D.; Poisson, J.; Zhang, Y. The I-TASSER Suite: Protein Structure and Function Prediction. *Nat Methods* **2015**, *12*, 7–8, doi:10.1038/nmeth.3213.
98. Humphrey, W.; Dalke, A.; Schulten, K. VMD: Visual Molecular Dynamics. *Journal of Molecular Graphics* **1996**, *14*, 33–38, doi:10.1016/0263-7855(96)00018-5.
99. Honorato, R.V.; Koukos, P.I.; Jiménez-García, B.; Tsaregorodtsev, A.; Verlato, M.; Giachetti, A.; Rosato, A.; Bonvin, A.M.J.J. Structural Biology in the Clouds: The WeNMR-EOSC Ecosystem. *Front. Mol. Biosci.* **2021**, *8*, 729513, doi:10.3389/fmolb.2021.729513.
100. van Zundert, G.C.P.; Rodrigues, J.P.G.L.M.; Trellet, M.; Schmitz, C.; Kastritis, P.L.; Karaca, E.; Melquiond, A.S.J.; van Dijk, M.; de Vries, S.J.; Bonvin, A.M.J.J. The HADDOCK2.2 Web Server: User-Friendly Integrative Modeling of Biomolecular Complexes. *Journal of Molecular Biology* **2016**, *428*, 720–725, doi:10.1016/j.jmb.2015.09.014.
101. Spagnuolo, L.; Della Posta, S.; Fanali, C.; Dugo, L.; De Gara, L. Antioxidant and Antiglycation Effects of Polyphenol Compounds Extracted from Hazelnut Skin on Advanced Glycation End-Products (AGEs) Formation. *Antioxidants (Basel)* **2021**, *10*, 424, doi:10.3390/antiox10030424.
102. Ardestani, A.; Yazdanparast, R. Cyperus Rotundus Suppresses AGE Formation and Protein Oxidation in a Model of Fructose-Mediated Protein Glycoxidation. *International Journal of Biological Macromolecules* **2007**, *41*, 572–578, doi:10.1016/j.ijbiomac.2007.07.014.
103. D'Introno, A.; Paradiso, A.; Scoditti, E.; D'Amico, L.; De Paolis, A.; Carluccio, M.A.; Nicoletti, I.; DeGara, L.; Santino, A.; Giovinazzo, G. Antioxidant and Anti-Inflammatory Properties of Tomato Fruits Synthesizing Different Amounts of Stilbenes. *Plant Biotechnology Journal* **2009**, *7*, 422–429, doi:10.1111/j.1467-7652.2009.00409.x.
104. Bottazzi, B.; Doni, A.; Garlanda, C.; Mantovani, A. An Integrated View of Humoral Innate Immunity: Pentraxins as a Paradigm. *Annu. Rev. Immunol.* **2010**, *28*, 157–183, doi:10.1146/annurev-immunol-030409-101305.
105. Hansson, G.K.; Hermansson, A. The Immune System in Atherosclerosis. *Nat Immunol* **2011**, *12*, 204–212, doi:10.1038/ni.2001.
106. Wang, N.; Liang, H.; Zen, K. Molecular Mechanisms That Influence the Macrophage M1â€"M2 Polarization Balance. *Front. Immunol.* **2014**, *5*, doi:10.3389/fimmu.2014.00614.
107. Dai, J.; Mumper, R.J. Plant Phenolics: Extraction, Analysis and Their Antioxidant and Anticancer Properties. *Molecules* **2010**, *15*, 7313–7352, doi:10.3390/molecules15107313.
108. Yu, W.; Tao, M.; Zhao, Y.; Hu, X.; Wang, M. 4'-Methoxyresveratrol Alleviated AGE-Induced Inflammation via RAGE-Mediated NF-KB and NLRP3 Inflammasome Pathway. *Molecules* **2018**, *23*, 1447, doi:10.3390/molecules23061447.
109. Khangholi, S.; Majid, F.A.A.; Berwary, N.J.A.; Ahmad, F.; Aziz, R.B.A. The Mechanisms of Inhibition of Advanced Glycation End Products Formation through Polyphenols in Hyperglycemic Condition. *Planta Med* **2016**, *82*, 32–45, doi:10.1055/s-0035-1558086.
110. Locati, M.; Curtale, G.; Mantovani, A. Diversity, Mechanisms, and Significance of Macrophage Plasticity. *Annu Rev Pathol* **2020**, *15*, 123–147, doi:10.1146/annurev-pathmechdis-012418-012718.
111. Deng, D.; Sun, P.; Yan, C.; Ke, M.; Jiang, X.; Xiong, L.; Ren, W.; Hirata, K.; Yamamoto, M.; Fan, S.; et al. Molecular Basis of Ligand Recognition and Transport by Glucose Transporters. *Nature* **2015**, *526*, 391–396, doi:10.1038/nature14655.
112. Kapoor, K.; Finer-Moore, J.S.; Pedersen, B.P.; Caboni, L.; Waight, A.; Hillig, R.C.; Bringmann, P.; Heisler, I.; Müller, T.; Siebeneicher, H.; et al. Mechanism of Inhibition of Human Glucose Transporter GLUT1 Is Conserved between Cytochalasin B and Phenylalanine Amides. *Proc. Natl. Acad. Sci. U.S.A.* **2016**, *113*, 4711–4716, doi:10.1073/pnas.1603735113.
113. Iancu, C.V.; Bocci, G.; Ishtikhar, M.; Khamrai, M.; Oreb, M.; Oprea, T.I.; Choe, J. GLUT3 Inhibitor Discovery through in Silico Ligand Screening and in Vivo Validation in Eukaryotic Expression Systems. *Sci Rep* **2022**, *12*, 1429, doi:10.1038/s41598-022-05383-9.
114. Christ, A.; Lauterbach, M.; Latz, E. Western Diet and the Immune System: An Inflammatory Connection. *Immunity* **2019**, *51*, 794–811, doi:10.1016/j.immuni.2019.09.020.
115. Younus, H.; Anwar, S. ANTIGLYCATING ACTIVITY OF ALOE VERA GEL EXTRACT AND ITS ACTIVE COMPONENT ALOIN. *Journal of Proteins & Proteomics* **2018**, *9*.

116. Santana, Á.L.; Macedo, G.A. Challenges on the Processing of Plant-Based Neuronutraceuticals and Functional Foods with Emerging Technologies: Extraction, Encapsulation and Therapeutic Applications. *Trends in Food Science & Technology* **2019**, *91*, 518–529, doi:10.1016/j.tifs.2019.07.019.
117. Cannizzaro, L.; Rossoni, G.; Savi, F.; Altomare, A.; Marinello, C.; Saethang, T.; Carini, M.; Payne, D.M.; Pisitkun, T.; Aldini, G.; et al. Regulatory Landscape of AGE-RAGE-Oxidative Stress Axis and Its Modulation by PPARγ Activation in High Fructose Diet-Induced Metabolic Syndrome. *Nutr Metab (Lond)* **2017**, *14*, 5, doi:10.1186/s12986-016-0149-z.
118. Espín, J.C.; García-Conesa, M.T.; Tomás-Barberán, F.A. Nutraceuticals: Facts and Fiction. *Phytochemistry* **2007**, *68*, 2986–3008, doi:10.1016/j.phytochem.2007.09.014.
119. Yeh, W.-J.; Hsia, S.-M.; Lee, W.-H.; Wu, C.-H. Polyphenols with Antiglycation Activity and Mechanisms of Action: A Review of Recent Findings. *J Food Drug Anal* **2017**, *25*, 84–92, doi:10.1016/j.jfda.2016.10.017.
120. Sang, S.; Shao, X.; Bai, N.; Lo, C.-Y.; Yang, C.S.; Ho, C.-T. Tea Polyphenol (-)-Epigallocatechin-3-Gallate: A New Trapping Agent of Reactive Dicarbonyl Species. *Chem Res Toxicol* **2007**, *20*, 1862–1870, doi:10.1021/tx700190s.
121. Jakopic, J.; Petkovsek, M.M.; Likozar, A.; Solar, A.; Stampar, F.; Veberic, R. HPLC–MS Identification of Phenols in Hazelnut (Corylus Avellana L.) Kernels. *Food Chemistry* **2011**, *124*, 1100–1106, doi:10.1016/j.foodchem.2010.06.011.
122. Grosso, G.; Yang, J.; Marventano, S.; Micek, A.; Galvano, F.; Kales, S.N. Nut Consumption on All-Cause, Cardiovascular, and Cancer Mortality Risk: A Systematic Review and Meta-Analysis of Epidemiologic Studies. *The American Journal of Clinical Nutrition* **2015**, *101*, 783–793, doi:10.3945/ajcn.114.099515.
123. Mayhew, A.J.; de Souza, R.J.; Meyre, D.; Anand, S.S.; Mente, A. A Systematic Review and Meta-Analysis of Nut Consumption and Incident Risk of CVD and All-Cause Mortality. *Br J Nutr* **2016**, *115*, 212–225, doi:10.1017/S0007114515004316.
124. Contini, M.; Baccelloni, S.; Frangipane, M.T.; Merendino, N.; Massantini, R. Increasing Espresso Coffee Brew Antioxidant Capacity Using Phenolic Extract Recovered from Hazelnut Skin Waste. *Journal of Functional Foods* **2012**, *4*, 137–146, doi:10.1016/j.jff.2011.09.005.
125. Bertolino, M.; Belviso, S.; Dal Bello, B.; Ghirardello, D.; Giordano, M.; Rolle, L.; Gerbi, V.; Zeppa, G. Influence of the Addition of Different Hazelnut Skins on the Physicochemical, Antioxidant, Polyphenol and Sensory Properties of Yogurt. *LWT - Food Science and Technology* **2015**, *63*, 1145–1154, doi:10.1016/j.lwt.2015.03.113.
126. Montella, R.; Coïsson, J.D.; Travaglia, F.; Locatelli, M.; Malfa, P.; Martelli, A.; Arlorio, M. Bioactive Compounds from Hazelnut Skin (Corylus Avellana L.): Effects on Lactobacillus Plantarum P17630 and Lactobacillus Crispatus P17631. *Journal of Functional Foods* **2013**, *5*, 306–315, doi:10.1016/j.jff.2012.11.001.
127. Caimari, A.; Puiggròs, F.; Suárez, M.; Crescenti, A.; Laos, S.; Ruiz, J.A.; Alonso, V.; Moragas, J.; del Bas, J.M.; Arola, L. The Intake of a Hazelnut Skin Extract Improves the Plasma Lipid Profile and Reduces the Lithocholic/Deoxycholic Bile Acid Faecal Ratio, a Risk Factor for Colon Cancer, in Hamsters Fed a High-Fat Diet. *Food Chemistry* **2015**, *167*, 138–144, doi:10.1016/j.foodchem.2014.06.072.
128. Ivanović, S.; Avramović, N.; Dojčinović, B.; Trifunović, S.; Novaković, M.; Tešević, V.; Mandić, B. Chemical Composition, Total Phenols and Flavonoids Contents and Antioxidant Activity as Nutritive Potential of Roasted Hazelnut Skins (Corylus Avellana L.). *Foods* **2020**, *9*, 430, doi:10.3390/foods9040430.
129. Peng, X.; Ma, J.; Chen, F.; Wang, M. Naturally Occurring Inhibitors against the Formation of Advanced Glycation End-Products. *Food Funct.* **2011**, *2*, 289, doi:10.1039/c1fo10034c.
130. Nagaraj, R.H.; Sarkar, P.; Mally, A.; Biemel, K.M.; Lederer, M.O.; Padayatti, P.S. Effect of Pyridoxamine on Chemical Modification of Proteins by Carbonyls in Diabetic Rats: Characterization of a Major Product from the Reaction of Pyridoxamine and Methylglyoxal. *Archives of Biochemistry and Biophysics* **2002**, *402*, 110–119, doi:10.1016/S0003-9861(02)00067-X.
131. Yoon, S.P.; Maeng, Y.H.; Hong, R.; Lee, B.R.; Kim, C.G.; Kim, H.L.; Chung, J.H.; Shin, B.C. Protective Effects of Epigallocatechin Gallate (EGCG) on Streptozotocin-Induced Diabetic Nephropathy in Mice. *Acta Histochemica* **2014**, *116*, 1210–1215, doi:10.1016/j.acthis.2014.07.003.

132. Cervantes-Laurean, D.; Schramm, D.D.; Jacobson, E.L.; Halaweish, I.; Bruckner, G.G.; Boissonneault, G.A. Inhibition of Advanced Glycation End Product Formation on Collagen by Rutin and Its Metabolites. *The Journal of Nutritional Biochemistry* **2006**, *17*, 531–540, doi:10.1016/j.jnutbio.2005.10.002.
133. Li, X.; Zheng, T.; Sang, S.; Lv, L. Quercetin Inhibits Advanced Glycation End Product Formation by Trapping Methylglyoxal and Glyoxal. *J. Agric. Food Chem.* **2014**, *62*, 12152–12158, doi:10.1021/jf504132x.
134. Mirza, R.E.; Fang, M.M.; Ennis, W.J.; Koh, T.J. Blocking Interleukin-1β Induces a Healing-Associated Wound Macrophage Phenotype and Improves Healing in Type 2 Diabetes. *Diabetes* **2013**, *62*, 2579–2587, doi:10.2337/db12-1450.
135. Hanhineva, K.; Törrönen, R.; Bondia-Pons, I.; Pekkinen, J.; Kolehmainen, M.; Mykkänen, H.; Poutanen, K. Impact of Dietary Polyphenols on Carbohydrate Metabolism. *IJMS* **2010**, *11*, 1365–1402, doi:10.3390/ijms11041365.
136. saponaro, A.; Porro, A.; Chaves-Sanjuan, A.; Nardini, M.; Rauh, O.; Thiel, G.; Moroni, A. Fusicoccin Activates KAT1 Channels by Stabilizing Their Interaction with 14-3-3- Proteins. *Plant Cell* **2017**, tpc.00375.2017, doi:10.1105/tpc.17.00375.